

Journal of Fish Biology

Plasticity of the skeleton and skeletal deformities in zebrafish (*Danio rerio*) linked to rearing density --Manuscript Draft--

Manuscript Number:	JFB-MS-19-0705R1
Full Title:	Plasticity of the skeleton and skeletal deformities in zebrafish (<i>Danio rerio</i>) linked to rearing density
Article Type:	Special Issue Regular Paper
Keywords:	deformities; plasticity; rearing density; skeleton; zebrafish
Corresponding Author:	Arianna Martini Universita degli Studi di Roma Tor Vergata Macroarea di Scienze Matematiche Fisiche e Naturali Rome, Rome ITALY
Corresponding Author Secondary Information:	
Corresponding Author's Institution:	Universita degli Studi di Roma Tor Vergata Macroarea di Scienze Matematiche Fisiche e Naturali
Corresponding Author's Secondary Institution:	
First Author:	Arianna Martini, PhD student
First Author Secondary Information:	
Order of Authors:	Arianna Martini, PhD student Huyseune Ann, Full Professor Witten P. Eckhard, Professor Boglione Clara, Senior Researcher
Order of Authors Secondary Information:	
Manuscript Region of Origin:	ITALY
Abstract:	<p>The teleost zebrafish (<i>Danio rerio</i>), an established model for human skeletal diseases, is reared under controlled conditions with defined parameters for temperature and photoperiod. Studies aimed at defining the proper rearing density have been performed with regard to behavioural and physiological stress response, sex ratio and reproduction. Studies concerning the effect of rearing density on the skeletal phenotype are lacking. This study is designed to analyse the response of the skeleton to different rearing densities and provides a description of the skeletal deformities. Wild type zebrafish were reared up to 30 dpf (days post-fertilization) in a common environment. From 30 to 90 dpf, animals were reared at three different densities: high density (HD) 32 fish/L, medium density (MD) 8 fish/L and low density (LD) 2 fish/L. Animals at 30 and 90 dpf were collected and whole-mount stained with Alizarin red S to visualise mineralized tissues. The entire skeleton was analysed for meristic counts and 172 types of deformities. The results showed that rearing density significantly influenced the specimens' average standard length, which decreased with increasing rearing density. Differences concerning meristic counts among the three groups were not observed. Rearing density-independent malformations affected the ribs, neural arches and the spines of the abdominal region as well as vertebrae of the caudal complex. The HD group showed the highest number of deformities per specimens, the highest number of observed types of deformities and, together with the MD group, the highest frequency of specimens affected by severe deformities. In particular, the HD group showed deformities affecting arches, spines and vertebral centra in the caudal region of the vertebral column. This study provides evidence of an effect of rearing density on the development of different skeletal phenotypes.</p>

Significance Statement:

The rearing density for zebrafish is often not reported in the literature. Inappropriate rearing density and small tank volumes are known to affect teleost skeletal development. This study shows that rearing density effects the body size and the skeletal phenotype in zebrafish. It is important to distinguish skeletal defects related to rearing condition from defects related to experimental conditions if zebrafish is used as a model to study skeletal development in teleosts or skeletal diseases in humans. This study provides an adaptable methodology for the assessment of skeletal malformations.

1 **Plasticity of the skeleton and skeletal deformities in zebrafish**
2 **(*Danio rerio*) linked to rearing density**

3 Martini Arianna^{1, 2}, Huysseune Ann², Witten P. Eckhard², Boglione
4 Clara¹.

5
6 ¹ Laboratory of Experimental Ecology and Aquaculture, Department
7 of Biology, University of Rome Tor Vergata, Rome, Italy

8 ² Laboratory of Evolutionary Developmental Biology, Department of
9 Biology, Gent University, Gent, Belgium

10
11 **Corresponding author:** Arianna Martini,
12 ariannamartini.89@gmail.com

13
14 **Funding information:** Martini A. acknowledges a grant from the
15 Doctorate School of the University of Rome Tor Vergata
16
17

Abstract

The teleost zebrafish (*Danio rerio*), an established model for human skeletal diseases, is reared under controlled conditions with defined parameters for temperature and photoperiod. Studies aimed at defining the proper rearing density have been performed with regard to behavioural and physiological stress response, sex ratio and reproduction. Studies concerning the effect of rearing density on the skeletal phenotype are lacking. This study is designed to analyse the response of the skeleton to different rearing densities and provides a description of the skeletal [deformities](#). Wild type zebrafish were reared up to 30 dpf (days post-fertilization) in a common environment. From 30 to 90 dpf, animals were reared at three different densities: high density (HD) 32 fish/L, medium density (MD) 8 fish/L and low density (LD) 2 fish/L. Animals at 30 and 90 dpf were collected and whole-mount stained with Alizarin red S to visualise [mineralized](#) tissues. The entire skeleton was analysed for meristic counts and 172 types of [deformities](#). The results showed that rearing density significantly influenced the specimens' average standard length, which decreased with increasing rearing density. Differences concerning meristic counts among the three groups were not observed. Rearing density-independent malformations affected the ribs, neural arches and the spines of the abdominal region as well as vertebrae of the caudal complex. The HD group showed the highest number of [deformities](#) per specimens, the highest number of observed types of [deformities](#) and, together with the MD group, the

43 highest frequency of specimens affected by severe deformities. In
44 particular, the HD group showed deformities affecting arches, spines
45 and vertebral centra in the caudal region of the vertebral column.

46 This study provides evidence of an effect of rearing density on the
47 development of different skeletal phenotypes.

48 Keywords: deformities, plasticity, rearing density, skeleton, zebrafish
49

Formatted: Line spacing: Double

Introduction

Phenotypic plasticity, a component of phenotypic variation (Klingenberg, 2019), is the ability of living organisms to respond to environmental or internal stimuli through changes in behaviour, morphology or physiology, producing different phenotypes. Phenotypic plasticity can be adaptive or non-adaptive, reversible or irreversible, and its type and degree are specific to the single trait and the environmental conditions involved. In an evolutionary perspective, phenotypic plasticity is a feature of the reaction norm of a trait of single organisms (i.e. the complete set of phenotypic responses of a trait to a specific environmental variable), that can be the target of natural selection, steering towards phenotypic accommodation and genetic assimilation (Pigliucci et al., 2006, Schmalhausen, 1949, Waddington, 1953; West-Eberhard, 2003, 2005).

Phenotypic plasticity is particularly relevant for skeletal tissues. The vertebrate skeleton is composed of five main different skeletal tissue types: notochord, cartilage, bone, dentin and enamel/enameloid. In teleosts, several intermediate tissue types are present and skeletal tissues are considered part of a continuum (Hall and Witten, 2019; Witten et al., 2010). They are able to respond to intrinsic and extrinsic cues (Roux, 1881; Ruff et al., 2006; Weinans and Prendergast, 1996; Wolff, 1892). Skeletal tissues and cells are plastic and dynamic throughout life as they modulate their structure in response to the mechanical load regime. The processes through

75 which the skeletal cells achieve modifications are modulation,
76 metaplasia, transdifferentiation and remodelling (Hall and Witten,
77 2007; Witten and Hall, 2015). The ability of tissues to modulate their
78 phenotype in response to mechanical load is known as "Wolff's law
79 of bone transformation" (Wolff, 1892) or as "bone functional
80 adaptation" (Ruff et al., 2006). A famous example is the two-legged
81 goat, whose hind limbs and thoracic skeleton became modified to
82 adapt to the bipedal gait (Slijper, 1942).

83 Examples of phenotypic plasticity of the teleost skeleton are
84 numerous. In cichlids, differences in the hardness or type of food
85 modify the jaw shape, the number and strength of jaw bone
86 trabeculae and the size of replacement teeth (Huysseune, 1994,
87 1995; Meyer, 1987). The mechanical load exerted by swimming
88 changes the shape of vertebral ~~bodies-centra~~ and can induce
89 lordosis in different teleost species (Kihara et al., 2002; Kranenbarg
90 et al., 2005). Forced swimming accelerates ossification rate of
91 vertebral bodies and cartilage formation in the head and the caudal
92 fin in zebrafish *Danio rerio* (Hamilton 1822) (Fiaz et al., 2012;
93 Suniaga et al., 2018; van der Meulen, 2005).

94 The rearing of fish implies the modification and control of several
95 environmental factors (e.g., photoperiod, temperature, type of diet,
96 diet composition, hydrodynamics) in order to optimize rearing
97 conditions in aquaculture or laboratory facilities. Aquaculture-related
98 research provides numerous examples of how modifications of
99 environmental conditions change the skeletal phenotype, including
100 the induction of skeletal ~~anomaliesdeformities~~.

101 In aquaculture, farming practices can be classified as intensive,
102 semi-intensive and extensive methodologies. They stand out for
103 several parameters, such as rearing density and tank volume,
104 hydrodynamics and diet. In intensive farming practice, rearing density
105 is high and tank volume smaller compared to semi-intensive and
106 extensive rearing conditions. The latter, besides being characterized
107 by decreased number of animal per volume and larger tanks, utilises
108 practises aimed at simulating the natural environment. This includes
109 differentiated hydrodynamics, and large live prey availability and
110 variety (Baluyut and Balnyme, 1995; Cataudella and Bronzi, 2001).
111 The above-mentioned rearing methodologies can affect the
112 morphology of the skeleton. In rainbow trout *Oncorhynchus mykiss*
113 (Walbaum 1792), the occurrence of skeletal anomalies-deformities
114 increases significantly in animals reared in intensive conditions
115 compared to animals reared in extensive conditions (Boglione et al.,
116 2014). Similar observations have been reported for advanced marine
117 teleosts: gilthead seabream (*Sparus aurata* L.) and red porgy
118 (*Pagrus pagrus* L.) reared in semi-intensive conditions showed a
119 lower number of skeletal deformities per individual and a lower
120 number of deformed individuals (Prestinicola et al., 2013; Roo et al.,
121 2010). Dusky grouper (*Epinephelus marginatus* Lowe 1834) larvae
122 reared in high-density conditions –at the highest stocking density
123 showed the highest frequency of deformed individuals, the highest
124 number of deformities per deformed individual, the largest range of
125 types of deformities and the highest incidence of individuals with at
126 least one severe deformity (Boglione et al., 2009).

127 *Danio rerio* is an established model organism in [biological](#) and
128 biomedical research and is now also used as a model for human
129 skeletal diseases. Insights into fundamental pathways of skeletal
130 formation and skeletal diseases can be obtained, provided the
131 differences between the teleost and mammalian skeleton are
132 considered (Witten et al., 2017). Laboratory zebrafish are reared
133 under controlled conditions, with defined parameters for temperature
134 and photoperiod, but recommendations for rearing densities differ
135 (Castranova et al., 2011) and standards based on experimental data
136 are lacking (Lawrence and Mason, 2012). The Zebrafish Book
137 (Westerfield, 2000) recommends a rearing density of 0.55 adult
138 fish/L, whereas the “Guide for the care and use of laboratory
139 animals” (Clark et al., 1997) and Matthews et al. (2002) recommend
140 5 to 10 individuals/L for adult fish. [Another published housing density](#)
141 [is 3.5 fish/L](#) (Tsang et al., 2017). Concerning rearing densities for
142 early life stages, published data range from 6.5, up to 94 fish/L
143 (Carvalho et al., 2006; Goolish et al., 1998; Matthews et al., 2002).
144 As Lawrence (2007) emphasized, “the classifications of densities in
145 zebrafish research tend to vary considerably depending on the
146 experimental setting”. Remarkably, studies about the effects of the
147 rearing density in *D. rerio* are scarce (Ribas et al., 2017). Published
148 data refer to the animals’ sex ratio (Liew et al., 2012; Ribas et al.,
149 2017), growth rate (Hazlerigg et al., 2012; Ribas et al., 2017), stress
150 and behavioural parameters (Ramsay et al., 2006; Shelton et al.,
151 2015) or reproductive rates (Goolish et al., 1998). The effect of
152 rearing densities on [the](#) skeleton and the onset of skeletal [deformities](#)

153 in this species has not been reported. The skeletal phenotype of
154 transgenic and mutant zebrafish lines for genes related to human
155 skeletal pathologies has already been extensively described (Fisher
156 et al., 2003; Gray et al., 2014; Gistelink et al., 2016; Haller et al.,
157 2018; Lleras Forero et al., 2018; Spoorendonk et al., 2008; Wopat et
158 al., 2018). Conversely, to our knowledge, the only works describing
159 the skeletal anomalies in wild type zebrafish are the study of age-
160 related deformities of Hayes et al. (2013) and a comprehensive
161 description of wild adult breeders and F1 juveniles *D. rerio* made by
162 Ferreri et al. (2000). The latter characterized 25 types of anomalies
163 affecting the vertebral column, vertebrae, fins and cranium.

164 The aim of this study was to analyse the response of the skeleton of
165 juvenile *D. rerio* to a single environmental variable, *i.e.* rearing
166 density. This study provides a description of skeletal deformities
167 developed in *D. rerio* reared at three different ~~stocking~~
168 during the juvenile stage.

169 **Materials and methods**

170 *Ethics statement*

171 All experiments were carried out at the Experimental Biology and
172 Aquaculture Laboratory, Università degli Studi di Roma Tor Vergata,
173 approved by the Animal-Welfare body and carried out in accordance
174 with Italian and European rules. All the animal experiments were
175 ethically approved and authorised by the General Director of the
176 Ministry of Health, Legislative Decree no.26/2014; European
177 Directive 2010/63/UE.

Formatted: Space After: 12 pt

178 *Specimens maintenance and collection*

179 All the specimens used in this study were obtained from the same
180 pool of AB line (commonly referred to as wild type, WT) zebrafish
181 breeders (n= 15), male:female ratio 1:2, housed in a 25 L aquarium
182 equipped with a bio-mechanical filter. Eggs were obtained by natural
183 spawning. Vital eggs were incubated at 28°C until hatching. After
184 hatching, the animals were transferred in one large aquarium at a
185 density of 20 animals/L and maintained there up to 30 days post-
186 fertilization (hereafter, dpf), a time point when a stable number of
187 individuals was achieved (Figure 1 SupplInfo). At 30 dpf, the
188 specimens were randomly divided into groups and reared at three
189 densities: i) high (32 fish/L), ii) medium (8 fish/L) and iii) low density
190 (2 fish/L) (hereafter referred to as HD, MD and LD, respectively). The
191 choice was based on the need to find a compromise between having
192 a sufficient number of fish for the analyses (especially for the MD and
193 LD group) and the rearing densities adopted usually in the zebrafish
194 facilities (5 fish/L for the adult stage). The remaining fish were
195 euthanized with a lethal dose (500 µl/L) of 2-phenoxyethanol and
196 fixed (1.5% glutaraldehyde and 1.5% paraformaldehyde in 0.1 M
197 cacodylate buffer, pH 7.4) representing a “time zero” sampling point
198 (hereafter referred to as T0).

199 The water used for all the tanks (breeders, eggs, larvae and
200 juveniles) was obtained mixing equal parts of water treated by
201 reverse osmosis water and 50 µm-filtered well water. The
202 photoperiod was 14L:10D and water parameters were maintained as

203 follows: water temperature 28°C, pH 6.8-8.5, water hardness 60-200
204 mg/L CaCO₃, nitrite and ammonia 0 mg/L, nitrate < 50 mg/L. Fish
205 were fed twice per day *ad libitum* with *Artemia salina* (L.) nauplii and
206 dry commercial food of different size according to the developmental
207 stages (Micron, Sera; Tetramin Baby, Junior and Flakes, Tetra®).

208 *Experimental system and samples collection*

209 The experimental rearing based on the three different density groups
210 lasted 60 days, from 30 to 90 dpf. The experimental rearing at the
211 three densities was carried out in a recirculating housing system
212 composed of nine interconnected 3.5 L trapezoidal tanks, equipped
213 with a mechanical/biological filter, air and water pumps. Water
214 exchange was 400 ml/min. Temperature, photoperiod and water
215 parameters were the same as reported above.

216 At the end of the experimental rearing, fish were ethanized and
217 fixed (as above). After 48 hours of fixation at 4°C, all the samples
218 were dehydrated in a graded ethanol series and stored in 70%
219 ethanol at 4°C until the analyses were performed.

220 The number of specimens used for the analyses was T0, n=32; HD,
221 n=65; MD, n=46 and LD, n=19.

222 *Staining*

223 Specimens were whole-mount stained for mineralized tissues with
224 Alizarin red S (modified from Taylor and Van Dyke, 1985). Samples
225 were first rehydrated in a graded ethanol series, washed in distilled
226 water and bleached with a 0.45% H₂O₂ and 0.5% KOH solution until

Formatted: Right: 0.79", Space After: 12 pt

227 the depigmentation was achieved, rinsed in distilled water and
228 transferred in saturated borax for 24h. Samples were then stained
229 with 0.01% Alizarin red S in 0.5% KOH overnight or longer, according
230 to the specimen's size, rinsed in distilled water, placed in 1% KOH for
231 2h, finally cleared and dehydrated in a graded series of KOH-glycerol
232 solutions and stored in 100% glycerol. The standard length (S_L , mm)
233 of individuals was then measured on digital images using the
234 software Fiji (Schindelin et al., 2012). Individuals were analysed for
235 meristic counts and skeletal anomalies using a Zeiss Axio Zoom V16
236 Stereo Zoom Microscope equipped with a 5MP CCD camera.

237 *Meristic counts and analyses of skeletal anomalies*

238 Meristic counts were carried out on the number of vertebrae of each
239 region of the vertebral column, fin rays of unpaired and paired (left
240 and right side) fins and their inner supports, and supraneural bones.
241 Nomenclature for skeletal elements follows Arratia et al. (2001) and
242 De Clercq et al. (2017). The vertebral column was subdivided into
243 four different regions, with nomenclature adapted from Bensimon-
244 Brito et al. (2012a). These authors combined the terminologies of
245 Arratia et al. (2001), Bird and Mabee (2003) and Nybelin (1963) as
246 follows: 1) Weberian region (vertebrae bearing the Weberian
247 ossicles), 2) abdominal region (rib-bearing vertebrae with open
248 haemal arches), 3) caudal region (vertebrae with closed haemal
249 arches) and 4) caudal complex (preurals and ural vertebrae with
250 modified haemal and neural arches and spines).

251 The use of the terms “anomaly”, “malformation” and “deformity”
252 follows Boglione et al. (2013) and Hennekam et al. (2013).
253 Malformations are early developmental defects; deformities are
254 defects that relate to later, epigenetic, factors. We reserve the use of
255 the term anomaly for the description of the methodology adopted in
256 this study and the cases for which nor “malformation” and
257 “deformation” can be used. Skeletal anomalies were classified using
258 an alphanumeric code (modified from Prestinicola et al., 2013),
259 where the capital letter indicates the affected skeletal region, the
260 numbers refer to the skeletal elements and the lowercase letters to
261 the types of anomalies (Table 1).

262 For each group (T0, HD, MD and LD), the following general metrics
263 were calculated: 1) frequency (%) of individuals with at least one
264 anomaly; 2) number of types of anomaly observed; 3) average
265 anomaly load (total number of anomalies recorded in a group/number
266 of malformed individuals per group); 4) frequency (%) of individuals
267 with at least one severe anomaly; 5) frequency (%) of observed
268 severe anomalies on the total number of observed anomalies; 6)
269 average severe anomaly load (number of severe anomalies/number
270 of individuals with severe anomalies); 7) frequency (%) of each- type
271 of anomaly, with respect to the total number of anomalies observed
272 in each group. In this paper, severe anomalies refer to those types of
273 anomalies that affect the vertebral axis (*i.e.*, scoliosis, lordosis,
274 kyphosis) and centra (deformation, elongation and reduction in
275 length, and fusion).

276 The phenotypic analysis of the skeleton was carried out based on
277 certain assumptions (adapted from Prestinicola et al., 2013): i) non-
278 completely fused vertebral centra were counted as distinct elements
279 in meristic counts while those completely fused as one; ii)
280 supernumerary bones with normal morphology were not considered
281 as anomalies but included as meristic count variations; conversely,
282 anomalous supernumerary elements were included among
283 anomalies; iii) upon simple visual inspection, only the identifiable
284 deformations in shape were considered as skeletal anomalies: if any
285 doubts arose, then the shape variation was not considered
286 anomalous; iv) curvatures of the vertebral column were considered
287 as scoliosis, lordosis and/or kyphosis only if the involved vertebral
288 centra were deformed, in order to exclude from the analyses axis
289 deformations due to neuromuscular anomalies or fixation artefacts.

290 *Statistical analyses*

291 Data obtained for the S_L and vertebrae counts were compared with
292 the Kruskal-Wallis test followed by Dunn's *post-hoc* test with the
293 Bonferroni correction.

294 Data obtained from the analysis of skeletal anomalies were used to
295 build a *Raw Matrix* (hereafter referred to as RM). The RM was
296 transformed into a *Binary Matrix* (hereafter named BM: presence of
297 each type of skeletal malformation = 1; absence = 0). RM was used
298 to calculate the frequencies (%) of each type of anomaly on the total
299 number of anomalies. The BM was used to calculate the frequencies
300 (%) of individuals affected by each type of anomaly in each group.

301 The frequencies obtained from the RM and the BM are presented
302 with tables or histograms. Statistical differences among groups were
303 tested with one-way PERMANOVA (9999 permutations) using both
304 the RM (Euclidean distance) and the BM (simple-matching) matrices.
305 RM and BM, and other matrices built on a subset of data were
306 subjected to Correspondence Analysis (CA) (Benzécri et al., 1973) in
307 order to visualize the relationships among groups and the role that
308 each anomaly plays in defining the characteristics of the different
309 groups.

310 Statistics was performed with the software Past 3.20 (Hammer et al.,
311 2001).

312 **Results**

313 *T0 group*

314 The average SL of the T0 specimens was 7.6 (± 1.7 SD) mm. All
315 caudal fin elements were identifiable in each T0 specimen. The
316 modal value and the range values of the T0 vertebral centra
317 (calculated excluding the specimens with vertebral centra still
318 mineralizing) were 34 and 32-35, respectively (Table 2).

319 The general metrics for the T0 group are summarised in Table 3. The
320 frequency of specimens affected by at least one anomaly and at least
321 one severe anomaly was 56% and 34%, respectively. The average
322 anomaly load (average number of anomalies per malformed
323 specimen) and the average severe anomaly load (average number of
324 severe anomalies per malformed specimen) was 9 and 2,
325 respectively. The number of observed types of anomalies was 17

326 (see Figure 1). Severe anomalies represented 12% of all anomalies.
327 Severe anomalies were represented by centra deformation (type
328 2def and elo/red) and scoliosis (1sco). The frequencies (%) of each
329 type of anomaly on the total number of anomalies counted in the T0
330 group and the frequency of the specimens affected by each anomaly
331 are reported in Figure 1. The most common (22-41% of T0
332 specimens) malformations were those affecting the neural arches of
333 the abdominal region (B4def) and the ribs (B7def), scoliosis in
334 vertebrae of the caudal complex (D1sco) and malformations of the
335 epural (G11def). No lordosis, kyphosis, nor fusions of vertebral
336 centra were recorded in the T0 individuals (except for one partial
337 fusion in the caudal complex vertebrae, D2par, in one fish).

338 *Experimental groups (HD, MD and LD)*

339 S_L significantly differed among groups (Kruskal-Wallis: $H=38.9$,
340 $p<0.001$). Specifically, $LD>MD>HD$ ($p<0.01$ for each pairwise Dunn's
341 test) (Figure 2).

342 The data referring to the meristic counts are shown in Table 2. The
343 modal value of the number of vertebral centra (= 33) and the inferior
344 lower limit of its range of variation (=30) were lower in the HD group
345 than in MD and LD group. This is due to the presence of specimens
346 affected by complete fusion of vertebral bodies-centra in the HD
347 group, as reported below.

348 Given that four types of malformation were commonly observed in
349 the T0 group (B4def, B7def, D1sco and G11def), these were
350 considered as "background malformations" for this zebrafish batch

Formatted: Not Highlight

351 when the experimental animals were analysed, and removed from
352 the analysis of the experimental groups. ~~Indeed~~Indeed, they occurred
353 at similar percentages in specimens of all experimental groups.

354 The general metrics referring to the analysis of the skeletal
355 anomalies for each group are presented in Table 4. The frequency
356 (%) of specimens with at least one skeletal anomaly was 100 in the
357 HD and LD groups and 98 the MD group (*i.e.* one specimen in the
358 MD group was only affected by some of the above-mentioned
359 “background malformations”). The highest average anomaly load
360 was found in the HD group (12 anomalies/malformed-deformed
361 specimen), as well as the widest variety of observed types of
362 anomalies (n=68). The highest frequencies of specimens with at least
363 one severe anomaly (73%) as of severe anomalies relative to the
364 total number of anomalies (21.4%) were observed in the MD group.

365 Statistically significant differences were found between the HD and
366 the other two experimental groups (MD and LD) (PERMANOVA,
367 $p < 0.01$). The frequencies (%) of deformities grouped per skeletal
368 element and per region, and the frequency of affected specimens are
369 represented in Figure 3 (raw data are provided in the Table_1_
370 SupplInfo), for each experimental group.

371 None of the following deformities was found in any experimental
372 group: lordosis in the Weberian, abdominal or caudal complex
373 regions (A1lor, B1lor and D1lor), kyphosis (code 1kyp), partial fusion
374 in the Weberian and abdominal region (A2par and B2par), elongated
375 vertebral centrum of the abdominal, caudal and caudal complex
376 regions (B2elo, C2elo and D2elo), demineralization of the urostyle

377 (D3dec), [deformities](#) of fin elements such as coracoid (code 20),
378 post-cleithrum (code 21), pectoral radials (E8sup/abs), pelvic
379 pterygiophores (L8abs and def) and rays (I12abs), anal
380 pterygiophores (F8sup) and rays (F12abs and def), dorsal
381 pterygiophores (H8abs, fus and dec) and rays (H12abs), epural
382 (G11sup) and caudal rays (G12sup), and cranial [deformities](#) such as
383 maxilla/premaxilla deformation (code 13), [deformations](#) of the
384 opercula (code 16) or branchiostegal rays (17sup, abs and def L),
385 neurocranium deformities (15) and saddle-back [syndrome](#) (1sbs).

386 The Weberian (code A) and abdominal vertebral (code B) regions
387 were the least affected skeletal regions in all the experimental groups
388 (see Table_1_ SupplInfo), with the exception of neural arches in the
389 Weberian vertebrae (malformation A4def) and supraneurals (A18
390 and A18sup).

391 The HD and MD groups showed the highest frequency of [deformities](#)
392 (Figure 3a) and frequency of individuals with [deformities](#) (Figure 3b)
393 affecting centra (Cc) and centra-associated elements of the caudal
394 region (Cae). In particular, the HD group showed the highest
395 percentage of individuals with [deformities](#) in the caudal region
396 (Figure 3b), both for centra-associated elements (Cae) (almost all the
397 C4 types and C5def, Figure 4b)-) and centra (Cc) (C2fus and def,
398 Figure 4b). ~~In t~~The MD ~~group, we described~~ the highest frequency of
399 [deformities](#) (Figure 4a) of the caudal vertebral centra (in particular
400 C2par) ~~was found~~. ~~Lastly,~~ Pectoral and anal fins were more
401 frequently deformed in the HD group.

402 The LD group showed the highest frequency of neural arch
403 deformities affecting the Weberian vertebrae (Aae in Figure 3, A4def
404 in the Table_1_SupplInfo) as well as the caudal fin elements (fin rays
405 and inner supports) (Figure 3). The LD group also displayed the
406 highest frequency of deformities affecting the centra of the caudal
407 complex, although the frequency of the specimens affected by these
408 deformities was higher in the MD group (Dc, Figure 3). Different from
409 HD and MD, some deformities were never present in the LD group,
410 *i.e.*, lordosis (C1lor), complete vertebral body-centra fusion (C2fus),
411 misplacement of the neural arch insertions (C4ins) and mismatched
412 fusion of neural and haemal spines (C4mis and C5mis), absence of
413 neural or haemal arches or spines (C4abs, C4abs R, C5abs) and
414 scoliosis (C1sco).

415 In Figure 5, examples of some of the deformities recorded are
416 provided.

417 *Correspondence Analysis (CA)*

418 Different CAs were performed on different matrices in order to
419 visualize the differences or relationships among samples and the role
420 each anomaly played in defining the characteristics of each group.

421 The CA applied to RM or BM, containing all the specimens and the
422 observed types of deformities (matrices 129 specimens x 86 types of
423 deformities). Note that one individual of the MD without any
424 deformities was not included in the matrix, since a null data vector,
425 *i.e.* a record for a specimen without anomalies, cannot be processed
426 by any of the techniques that require vector normalisation, e.g. by

Formatted: Right: 0.79", Space After: 12 pt

427 correspondence analysis. The CA applied to RM and BM gave
428 ordination models exhibiting a very low variance for the first three
429 axes (14% and 13%, respectively). Therefore, they are not shown. CA
430 was next applied to a subset of data obtained from the RM containing
431 19 randomly sampled individuals per group. This number of samples
432 was chosen on the base of the sample size of the LD group, in order
433 to avoid bias due to differences in the sample's dimension. The final
434 matrix was 57 specimens x 12 descriptors. The CA explained an
435 overall variance of 55% for the first three axes of correspondences.
436 In Figure 6, the ordination model obtained on CA1 and CA2 axes
437 (explaining 43% of the variance) is shown for each group on different
438 graphs. The HD centroid plots on the 3rd quadrant (negative semi-
439 plane of CA1), where the deformities of the centra-associated
440 elements (Bae and Cae) and vertebral centra (Bc and Cc) of the
441 abdominal and caudal regions are located. The MD and LD centroids
442 are positioned in the positive half-space of CA 1, with MD in an
443 intermediate position with respect to HD and LD groups. Most
444 individuals of the MD and LD groups are located in the 1st quadrant,
445 overlapping with malformations of the associated elements of the
446 Weberian vertebrae and of the pectoral and caudal fins. In all groups,
447 only a few specimens of the three experimental groups were
448 positioned in the 4th quadrant, where deformities of the anal and
449 dorsal fins and associated elements of the caudal complex vertebrae
450 are situated.

451 **Discussion**

452 ~~In~~ this paper, ~~we described~~ describes the phenotypic plasticity of
453 the skeleton and the occurrence of skeletal deformities in wild-type
454 *D. rerio* reared under identical conditions, with rearing densities being
455 the only variable. Our results reveal (1) the presence of certain
456 anomalies in zebrafish of different age and experiencing different
457 experimental conditions (T0, HD, MD and LD), (2) a significant
458 difference in size (S_L) depending on rearing densities, and (3) a
459 higher incidence of deformities of vertebrae of the caudal region in
460 animals reared at higher densities, in particular deformities of arches
461 and spines and fusion of vertebral bodiescentra, discussed below.

462 *Rearing density-independent skeletal malformations: the starting*
463 *point (T0)*

464 Animals at the same age (30 dpf), but of different sizes (S_L), show
465 that skeletal development is more advanced in larger individuals
466 compared to smaller individuals. This confirms the findings in
467 previous studies that show a better correlation of skeletal
468 development with size than with age, in *D. rerio* (Cubbage and
469 Mabee, 1996; Parichy *et al.*, 2009) and in farmed fish, *i.e.* Atlantic
470 halibut (*Hippoglossus hippoglossus* L.) (Sæle and Pittman, 2010).

471 The analysis of the skeletal phenotype at the beginning of the
472 experiment allowed identifying malformations of the ribs (B7def), and
473 neural arches and spines in the abdominal region (B4def), scoliosis
474 in the caudal complex (D1sco) and malformations of the epural
475 (G11def) as “background malformations” for the zebrafish used in
476 this study. The presence of malformed ribs and neural arches of the

477 abdominal region reported in the present work is in agreement with
478 the study of Ferreri et al. (2000). In their work, reared specimens
479 displayed a higher frequency of individuals affected by the
480 aforementioned malformations than wild zebrafish sampled from the
481 river Ganges. Even in wild specimens, about 13% of ribs and 21% of
482 neural arches and spines (although not assigned to distinct regions)
483 were diagnosed as malformed. The high incidence of malformations
484 of neural arches and spines in the abdominal region (close to 100%
485 of the analysed specimens) and the presence of malformed ribs
486 (ranging from 39 to 80%) was also reported for *O. mykiss* reared
487 both at low and high densities (Boglione *et al.*, 2014). Thus, similar to
488 *O. mykiss*, *D. rerio* appears to be susceptible to develop these
489 particular malformations.

490 Other malformations were found to be present with low frequencies
491 in the T0 specimens, e.g., malformations of the caudal complex, *i.e.*
492 D1sco (22%), D3def (6%), D4def5 (13%), and D2def (13%).
493 Interestingly, no fusions were detected, except for a single
494 occurrence in the caudal complex (D2par). It is recognised that the
495 vertebrae of the caudal complex display a high degree of plasticity
496 and its predisposition to develop vertebral body-centra fusions is well
497 documented at least in some species (Bensimon-Brito et al., 2010,
498 2012b; Gavaia et al., 2002; Koumoundourous et al., 1997,
499 Prestinicola et al., 2013; Witten et al., 2006). As part of normal
500 development, the last vertebral body – the urostyle – in zebrafish
501 forms through five fusion events (Bensimon-Brito et al., 2010,
502 2012b). The preural vertebral centra, which frequently possess an

503 accessory arch, show a higher tendency to fuse than the vertebrae of
504 the anteriormost regions (Bensimon-Brito et al., 2012b; Eastman,
505 1980).

506 *Effects of the rearing densities*

507 Specimens reared at high density (HD) showed a significantly
508 reduced growth with respect to the specimens reared at medium and
509 low densities. An inverse relation between growth and rearing density
510 has also been described for zebrafish reared from 6 to 90 dpf at 19,
511 37 and 74 fish/L (Ribas et al., 2017), as well for other basal teleost
512 species such as *O. mykiss*, and for advanced teleosts such as *H.*
513 *hippoglossus* and discus (*Symphysodon aequifasciatus* Pellegrin
514 1904) (Björnsson, 1994; Holm et al., 1990; Tibile et al., 2016). It has
515 been proposed that size differences relate to the reduction in feeding
516 activity or to an increase in energy expenditure associated with
517 enhanced swimming activity due to increased competition or
518 interactions. In our experimental rearing, food was administered *ad*
519 *libitum*, consequently, insufficient feeding was unlikely a causative
520 factor for the reduced size in the specimens reared at higher
521 densities.

522 Rearing at different densities after 30 dpf did not influence the modal
523 values of meristic characters. Lower mean values and lower limit of
524 the variation range for the number of vertebral centra observed in the
525 HD reared zebrafish related to the presence of complete vertebral
526 ~~bodies-centra~~ fusions (which in the meristic counts were accounted
527 as one element). Ferreri et al. (2000) compared wild and reared

528 zebrafish and found similar ranges of variation for several meristic
529 elements, with the exception of the anal and pectoral fin rays. Bird
530 and Mabee (2003) confirmed what ~~was previously reported by Ferreri~~
531 ~~et al. (2000)~~Ferreri et al. (2000) previously reported for vertebral
532 centra counts even in other reared zebrafish. Usually, variation in the
533 number of meristic elements is due to changes in environmental
534 conditions during the early developmental stages. For example, low
535 temperatures lead to an increased number of vertebrae in reared
536 zebrafish (Sfakianakis et al., 2011).

537 All the specimens analysed (with one exception in the MD group,
538 already discussed) showed at least one anomaly (Table 4). Such a
539 high frequency may be surprising but has been reported before. High
540 frequencies of zebrafish affected by at least one anomaly were
541 already reported for both wild (87%) and reared (93%) specimens by
542 Ferreri et al. (2000).

543 The HD group displayed the highest average number of deformities
544 per specimen and a larger variety of types of deformities. The latter
545 could be a density effect but it could also relate to the larger number
546 (n = 65) of HD specimens with respect to the MD (n = 46) and LD (n
547 = 19) groups. However, the highest average number of deformities
548 per specimen, as detected in the HD group, parallels what has been
549 already described in aquaculture facilities. Semi-intensive rearing
550 methodologies (characterized also by reduced rearing densities)
551 compared to intensive rearing conditions, decrease the occurrence of
552 skeletal deformities in farmed fish (Boglione et al., 2009; Prestinicola
553 et al., 2013; Zouiten et al., 2011). Similar to what has been described

554 for an advanced teleost, the *E. marginatus* (Boglione et al., 2009),
555 rearing density alone can affect the skeletal phenotype in zebrafish,
556 and increases the occurrence of particular types of deformities in the
557 caudal region of the vertebral column (partial and complete fusions of
558 vertebral bodiescentra, deformation of neural and haemal arches).
559 The susceptibility of the caudal region to deformities has been
560 already described in farmed Atlantic salmon (*Salmo salar* L.).
561 Vertebral centra compressions and fusions can relate to high-
562 temperature exposure during the embryonic stages (Grini et al.,
563 2011). The aggravation of such deformities in salmonids reared at
564 high temperature can occur later, for example during the late juvenile
565 seawater phase (Wargelius et al., 2015). The latter may be the result
566 of a synergic effect of the rearing temperature and the high density
567 used during the seawater rearing. Vertebral centra deformities in
568 Atlantic salmon have also been attributed to other not fully elucidated
569 causative factors acting during later ontogenetic stages (Fjellidal, et
570 al., 2007, Fjellidal et al., 2012).

571 The skeletal elements that displayed the most distinct phenotypic
572 response to increased rearing density were neural and haemal
573 arches and spines (deformations in shape, C4def and C5def),
574 followed by centra of the caudal region (C2par and fus).

575 Despite the fact that anomalies of arches and spines were also
576 observed in a few specimens of the T0 group, their frequency, and
577 that of specimens affected, are far higher in the HD than in the LD
578 group. Vertebral centra and arches in teleosts are different
579 developmental modules. Vertebral centra originate as chordacentra

580 by mineralization of the notochord sheath, whilst the associated
581 elements arches and spines are patterned by the somites (Laerm,
582 1979, Fleming et al., 2015). The duality in vertebral column elements'
583 formation could explain the higher incidence of deformities of arches
584 and spines compared to vertebral centra, in the HD group.
585 Interestingly, malformations, similar to those shown in Fig. 5c, have
586 been described for fused somite mutant zebrafish (tbx6 mutation)
587 (van Eedden et al., 2006, Fleming et al., 2004). In this mutant
588 zebrafish line, the somitogenesis is disturbed and the specimens
589 show malformations of arches and spines, but separated vertebral
590 centra. That shows that centra and associate elements are two
591 distinct developmental modules. However, the mechanisms by which
592 rearing density induces late vertebral column deformities that
593 resemble mutant-related malformations remain to be elucidated.
594 Deformities of arches and spines have also been related to
595 musculature impairments (Favaloro et al., 2006, Backiel et al., 1984).
596 Behavioural studies on *O. mykiss* reared at high stocking densities
597 (Bégout Anras and Lagardère, 2004; Cooke et al., 2000) showed that
598 the complexity of swimming trajectories, space utilization and activity
599 rhythms were altered and that swimming activity, oxygen
600 consumption and muscular activity increased when compared with
601 individuals reared at lower densities. Moreover, the crowded
602 conditions augmented the occurrence of changes in swimming
603 direction with sharper turning angles with respect to individuals kept
604 at lower densities (Bégout Anras and Lagardère, 2004). The
605 swimming patterns suggested recurring avoidance behaviours of

606 individuals held in the same tank. Avoidance behaviours imply the
607 utilization of fast C-start movements, usually occurring during escape
608 responses, which start with the contraction of the muscles of one
609 side of the body, at the level of the individual's centre of mass ~~(the~~
610 ~~central region of fish body)~~, in which the propulsive force develops,
611 allowing the fish to change orientation (Eaton and Emberley, 1991).

612 During the fast start movements, the body bends at the level of the
613 central region, below the dorsal fin, at the 50% of the fish T_L as
614 shown for zebrafish by Danos and Lauder (2012). In *Cyprinus carpio*
615 the maximum vertebral column curvature has been calculated to be
616 between 50 and 80% of fish T_L (Shadwick and Lauder, 2006).

617 During fast start movements, the muscles generate a mechanical
618 load on the flexing vertebral column (Shadwick and Lauder, 2006;
619 Wakeling and Johnston, 1999).

620 Mechanical loading increases bone formation in zebrafish (Fiaz et al.,
621 2010; Suniaga et al., 2018) especially if its frequency is high and the
622 mechanical load is dynamic, rather than static (Lisková and Hert,
623 1971; Rubin and McLeod, 1994; Turner, 1998; Turner et al., 1994a,b;
624 Turner et al., 1995).

625 Therefore, if a crowded environment leads to an increased number of
626 interactions between animals and thus changes in swimming
627 trajectories, for example due to food competition, possibly, the centra
628 of the central region (*viz.* caudal) of animals reared at higher
629 densities are more often subjected to the bendings, moments
630 generated by the axial musculature. The C-shaped bending of an
631 elongated structure, such as the vertebral column, produces

Formatted: Not Strikethrough, Not Highlight

Formatted: Not Highlight

Formatted: Not Highlight

Formatted: Not Strikethrough, Not Highlight

632 compression on the concave side and strain on convex one. Thus,
633 the intervertebral space on the concave side of the bending would be
634 subjected to compression, i.e. mechanical loading. Indeed, the
635 concave and convex sides can reverse from fast movement to
636 another, according to the turning direction. This increased elicitation
637 could explain the occurrence of fusion in the caudal region of the
638 vertebral column.

639 In this study, the complete fusion of vertebral bodies-centra (C2fus)
640 was never observed in specimens reared at low density. Partial
641 fusions (C2par) occurred at a lower frequency in LD compared to the
642 HD and MD groups. Ferreri et al. (2000), using densities far lower
643 than the LD used in this work, did not record vertebral fusion,
644 suggesting that their occurrence and severity could be linked to the
645 increased rearing density. Vertebral body-centra fusion can develop
646 at various time points during development. Very early fusions in
647 zebrafish relate to the ectopic mineralisation of the notochord sheath
648 in prospective intervertebral regions (Bensimon-Brito et al., 2012b). It
649 is unlikely that this type of very early fusions accounts for
650 observations made in this experiment: notochord segmentation takes
651 place during early ontogeny and it would not explain differences in
652 the occurrence of vertebral fusions in animals reared at different
653 rearing densities during the juvenile period when the vertebral centra
654 identity is already determined. Further, animals from the T0 group did
655 not show fused vertebrae.

656 The next (early) process that can cause the fusion of vertebral bodies
657 centra in zebrafish is the bridging of intervertebral spaces by bone

658 that develops around the mineralised notochord sheath (Bensimon-
659 Brito et al., 2012b; Ytteborg et al., 2010). A third process that may
660 lead to a late fusion (not described in zebrafish but in *S. salar*), is
661 caused by metaplasia, *i.e.* osteoblasts of the vertebral endplate
662 growth zone turn in cells with a chondroblast-like phenotype,
663 producing cartilage in the intervertebral space. This ectopic cartilage
664 later mineralizes and is subsequently remodelled into bone (Fjellidal
665 et al., 2012; Witten et al., 2005; 2006; Ytteborg et al., 2010).

666 In conclusion, our study shows the effect of rearing density on the
667 growth rate of zebrafish and provides evidence that rearing density
668 affects the skeletal phenotype in this species. High and, to some
669 extent, medium rearing densities slowed down growth and induced
670 deformities, particularly in the caudal region of the vertebral column.
671 Our results suggest that a density of 2 fish/litre, between the age of
672 30 and 90 dpf can help to reduce the incidence of skeletal
673 malformations in *D. rerio*. This is especially relevant if zebrafish is
674 used for studying skeletal pathologies. Moreover, for this analysis,
675 we propose a methodology that is adaptable and can be used in
676 various contexts to assess skeletal malformations–anomalies in
677 zebrafish or other species. For example, the alphanumeric code
678 used here can be adapted to different levels of details according to
679 the needs or applications (*i.e.*, by grouping different types of
680 malformations, or by adding subcodes for peculiar or different types
681 of malformations). Such standardization may facilitate comparison
682 among different studies.

683 **Acknowledgements:**

684 We are grateful to A. Forlino for providing the zebrafish breeders
685 used in this study. This research is a part of the Ph.D. thesis of
686 Arianna Martini.

687 **Author contributions:** CB and PEW conceived the experimental
688 design, AM carried out the experiments, performed the analyses and
689 elaborated the data; AM, AH, PEW and CB discussed the results and
690 wrote the paper. All authors have approved the final version of the
691 manuscript.

692 **References**

693 Arratia, G., Schultze, H. P. & Casciotta, J. (2001). Vertebral column
694 and associated elements in dipnoans and comparison with other
695 fishes: development and homology. *Journal of Morphology*,
696 **250**(2), 101-172

697 Backiel, T., Kokurewicz, B., & Ogorzałek, A. (1984). High incidence
698 of skeletal anomalies in carp, *Cyprinus carpio*, reared in cages in
699 flowing water. *Aquaculture*, **43**(4), 369-380.

700 Baluyut, E. & Balnyme, E. (1995). *Aquaculture systems and*
701 *practices: a selected review*. Daya Books

702 Bégout Anras, M.L. & Lagardère, J. P. (2004). Measuring cultured
703 fish swimming behaviour: first results on rainbow trout using
704 acoustic telemetry in tanks. *Aquaculture*, **240**(1-4), 175-186.

705 Bensimon-Brito, A., Cancela, M. L., Huysseune, A., & Witten, P. E.
706 (2010). The zebrafish (*Danio rerio*) caudal complex - a model to

707 study vertebral body fusion. *Journal of Applied Ichthyology*, **26**(2),
708 235–238.

709 Bensimon-Brito, A., Cardeira, J., Cancela, M. L., Huisseune, A., &
710 Witten, P. E. (2012a). Distinct patterns of notochord mineralization
711 in zebrafish coincide with the localization of Osteocalcin isoform 1
712 during early vertebral centra formation. *BMC developmental*
713 *Developmental Biology*, **12**(28), [https://doi.org/10.1186/1471-](https://doi.org/10.1186/1471-213X-12-28)
714 [213X-12-28](https://doi.org/10.1186/1471-213X-12-28).

715 Bensimon-Brito, A., Cancela, M. L., Huisseune, A., & Witten, P. E.
716 (2012b). Vestiges, rudiments and fusion events: the zebrafish
717 caudal fin endoskeleton in an evo-devo perspective. *Evolution &*
718 *Development*, **14**(1), 116–127.

719 Benzécri, J. P. (1973). *L'analyse des données* (Vol. 2, p. I). Paris:
720 Dunod.

721 Bird, N. C., & Mabee, P. M. (2003). Developmental morphology of
722 the axial skeleton of the zebrafish, *Danio rerio* (Ostariophysi:
723 Cyprinidae). *Developmental dynamics*, **228**(3), 337-357.

724 Björnsson, B. (1994). Effects of stocking density on growth rate of
725 halibut (*Hippoglossus hippoglossus* L.) reared in large circular
726 tanks for three years. *Aquaculture*, **123**(3-4), 259-270.

727 Boglione, C., Marino, G., Giganti, M., Longobardi, A., De Marzi, P., &
728 Cataudella, S. (2009). Skeletal anomalies in dusky grouper
729 *Epinephelus marginatus* (Lowe 1834) juveniles reared with
730 different methodologies and larval densities. *Aquaculture*, **291**(1–
731 2), 48–60.

Formatted: Font: Italic

732 Boglione, C., Gisbert, E., Gavaia, P., Witten, P. E., Moren, M.,
733 Fontagné, S., & Koumoundouros, G. (2013). Skeletal anomalies in
734 reared European fish larvae and juveniles. Part 2: main typologies,
735 occurrences and causative factors. *Reviews in Aquaculture*, 5,
736 S121-S167.

Formatted: Italian (Italy), Not Highlight

Formatted: Italian (Italy)

737 Boglione, C., Pulcini, D., Scardi, M., Palamara, E., Russo, T., &
738 Cataudella, S. (2014). Skeletal anomaly monitoring in rainbow
739 trout (*Oncorhynchus mykiss*, Walbaum 1792) reared under
740 different conditions. *PloS one*, 9(5), e96983
741 <https://doi.org/10.1371/journal.pone.0111294>.

742 Carvalho, A. P., Araújo, L., & Santos, M. M. (2006). Rearing
743 zebrafish (*Danio rerio*) larvae without live food: evaluation of a
744 commercial, a practical and a purified starter diet on larval
745 performance. *Aquaculture Research*, 37(11), 1107-1111.

746 Castranova, D., Lawton, A., Lawrence, C., Baumann, D. P., Best, J.,
747 Coscolla, J., Doherty, A., Ramos, J., Hakkesteeg, J., Wang, C.,
748 Wilson, J., Malley, J., & Wilson, C. (2011). The effect of stocking
749 densities on reproductive performance in laboratory zebrafish
750 (*Danio rerio*). *Zebrafish*, 8(3), 141-146.

751 Cataudella, S., & Bronzi, P. (2001). *Acquacoltura Responsabile:*
752 *verso le produzioni acquatiche del terzo millennio*. Unimar -
753 Uniprom.

754 Clark, J. D., Gebhart, G. F., Gonder, J. C., Keeling, M. E., & Kohn, D.
755 F. (1997). The 1996 guide for the care and use of laboratory
756 animals. *ILAR journal*, 38(1), 41-48.

757 Cooke, S. J., Chandroo, K. P., Beddow, T. A., Moccia, R. D., &
758 McKinley, R. S. (2000). Swimming activity and energetic
759 expenditure of captive rainbow trout *Oncorhynchus mykiss*
760 (Walbaum) estimated by electromyogram telemetry. *Aquaculture*
761 *Research*, **31**(6), 495-505.

762 Cubbage, C. C., & Mabee, P. M. (1996). Development of the cranium
763 and paired fins in the zebrafish *Danio rerio* (Ostariophysi,
764 Cyprinidae). *Journal of Morphology*, **229**(2), 121–160.

765 Danos, N., & Lauder, G. V. (2012). Challenging zebrafish escape
766 responses by increasing water viscosity. *Journal of Experimental*
767 *Biology*, **215**(11), 1854-1862.

768 De Clercq, A., Perrott, M. R., Davie, P. S., Preece, M. A., Wybourne,
769 B., Ruff, N., Huysseune, A., & Witten, P. E. (2017). Vertebral
770 column regionalisation in Chinook salmon, *Oncorhynchus*
771 *tshawytscha*. *Journal of anatomy*, **231**(4), 500-514.

772 Eastman, J. (1980). The caudal skeletons of catostomid fishes.
773 *American Midland Naturalist*, 133–148.

774 Eaton, R. C., & Emberley, D. S. (1991). How stimulus direction
775 determines the trajectory of the Mauthner-initiated escape
776 response in a teleost fish. *Journal of Experimental Biology*, **161**(1),
777 469-487.

778 Favaloro, E., & Mazzola, A. (2006). Meristic character counts and
779 incidence of skeletal anomalies in the wild *Diplodus puntazzo*
780 (Cetti, 1777) of an area of the south-eastern Mediterranean Sea.
781 *Fish Physiology and Biochemistry*, **32**(2), 159-166.

Formatted: Font: Italic

Formatted: Font: Italic

Formatted: Font: Bold

- 782 Ferreri, F., Nicolais, C., Boglione, C., & Bertolini, B. (2000). Skeletal
783 characterization of wild and reared zebrafish: anomalies and
784 meristic characters. *Journal of Fish Biology*, **56**(5), 1115-1128.
- 785 Fiaz, A. W., Léon-Kloosterziel, K. M., Gort, G., Schulte-Merker, S.,
786 van Leeuwen, J. L., & Kranenbarg, S. (2012). Swim-training
787 changes the spatio-temporal dynamics of skeletogenesis in
788 zebrafish larvae (*Danio rerio*). *PLoS One*, **7**(4), e34072.
789 <https://doi.org/10.1371/journal.pone.0034072>.
- 790 Fiaz, A. W., van Leeuwen, J. L., & Kranenbarg, S. (2010).
791 Phenotypic plasticity and mechano-transduction in the teleost
792 skeleton. *Journal of Applied Ichthyology*, **26**(2), 289–293.
- 793 Fisher, S., Jagadeeswaran, P., & Halpern, M. E. (2003).
794 Radiographic analysis of zebrafish skeletal defects.
795 *Developmental Biology*, **264**(1), 64–76.
- 796 Fjellidal, P. G., Hansen, T., Breck, O., Ørnstrud, R., Lock, E.-J.,
797 Waagbø, R., Wargelius, A., & Witten, P. E. (2012). Vertebral
798 deformities in farmed Atlantic salmon (*Salmo salar* L.) - etiology
799 and pathology. *Journal of Applied Ichthyology*, **28**(3), 433–440.
- 800 Fjellidal, P. G., Hansen, T. J., & Berg, A. E. (2007). A radiological
801 study on the development of vertebral deformities in cultured
802 Atlantic salmon (*Salmo salar* L.). *Aquaculture*, **273**(4), 721–728.
- 803 [Fleming, A., Keynes, R., & Tannahill, D. \(2004\). A central role for the](#)
804 [notochord in vertebral patterning. *Development*, **131**\(4\), 873-880.](#)
- 805 [Fleming, A., Kishida, M. G., Kimmel, C. B., & Keynes, R. J. \(2015\).](#)
806 [Building the backbone: the development and evolution of vertebral](#)
807 [patterning. *Development*, **142**\(10\), 1733-1744.](#)

Formatted: Font: Italic

Formatted: Font: Bold

808 Gavaia, P. J., Dinis, M. T., & Cancela, M. L. (2002). Osteological
809 development and abnormalities of the vertebral column and caudal
810 skeleton in larval and juvenile stages of hatchery-reared Senegal
811 sole (*Solea senegalensis*). *Aquaculture*, **211**(1-4), 305-323.

812 Gistelincx, C., Witten, P. E., Huysseune, A., Symoens, S., Malfait, F.,
813 Larionova, D., Pascal Simoens, P., Dierick, M., Van Hoorebeke,
814 L., De Paepe, A., Kwon, R.Y., Weis, M., Eyre, D., R., Willaert, A.,
815 & Coucke, P.J. (2016). Loss of Type I Collagen Telopeptide Lysyl
816 Hydroxylation Causes Musculoskeletal Abnormalities in a
817 Zebrafish Model of Bruck Syndrome. *Journal of Bone and Mineral*
818 *Research*, **31**(11), 1930–1942.

819 [Grimi, A., Hansen, T., Berg, A., Wargelius, A., & Fjelldal, P. G. \(2011\).](#)
820 [The effect of water temperature on vertebral deformities and](#)
821 [vaccine-induced abdominal lesions in Atlantic salmon, *Salmo salar*](#)
822 [L. *Journal of fish diseases*, **34**\(7\), 531-546.](#)

823 Goolish, E. M., Evans, R., Okutake, K., & Max, R. (1998). Chamber
824 volume requirements for reproduction of the zebrafish *Danio rerio*.
825 *The Progressive fish-culturist*, **60**(2), 127-132.

826 Gray, R. S., Wilm, T. P., Smith, J., Bagnat, M., Dale, R. M.,
827 Topczewski, J., Johnson, S.L., & Solnica-Krezel, L. (2014). Loss of
828 col8a1a function during zebrafish embryogenesis results in
829 congenital vertebral malformations. *Developmental Biology*,
830 **386**(1), 72–85.

831 Hall, B. K., & Witten, P. E. (2007). Plasticity of and transitions
832 between skeletal tissues in vertebrate evolution and development.
833 *Major transitions in vertebrate evolution*, 13-56.

834 Hall, B.K., & Witten, P.E. (2019). Plasticity and Variation of Skeletal
835 Cells and Tissues and the Evolutionary Development of
836 Actinopterygian Fishes. In: Z., Johanson, C., Underwood, M.,
837 Richter (Eds.) *Evolution and Development of Fishes* (pp. 126-143).
838 Cambridge University Press, Cambridge.

839 Haller, G., McCall, K., Jenkitkasemwong, S., Sadler, B., Antunes, L.,
840 Nikolov, M., Whittle, J., Upshaw, Z., Shin, J., Baschal, E.,
841 Cruchaga, C., Harms, M., Raggio, C., Morcuende, J.A.,
842 Giampietro, P., Miller, N.H., Wise, C., Gray, R.S., Solnica-Krezel,
843 L., Knutson, M., Dobbs, M.B., & Gurnett, C. A. (2018). A missense
844 variant in SLC39A8 is associated with severe idiopathic scoliosis.
845 *Nature Communications*, **9**(1), [https://doi.org/10.1038/s41467-018-](https://doi.org/10.1038/s41467-018-06705-0)
846 [06705-0](https://doi.org/10.1038/s41467-018-06705-0).

847 Hammer, Ø., Harper, D. A., & Ryan, P. D. (2001). PAST:
848 paleontological statistics software package for education and data
849 analysis. *Palaeontologia electronica*, **4**(1), 9.

850 Hayes, A. J., Reynolds, S., Nowell, M. A., Meakin, L. B., Habicher, J.,
851 Ledin, J., Bashford, A., Caterson, B., & Hammond, C. L. (2013).
852 Spinal deformity in aged zebrafish is accompanied by
853 degenerative changes to their vertebrae that resemble
854 osteoarthritis. *PLoS ONE*, **8**(9), 1–12.

855 Hazlerigg, C. R., Lorenzen, K., Thorbek, P., Wheeler, J. R., & Tyler,
856 C. R. (2012). Density-dependent processes in the life history of
857 fishes: evidence from laboratory populations of zebrafish *Danio*
858 *rerio*. *PLoS One*, **7**(5), e37550.
859 <https://doi.org/10.1371/journal.pone.0037550>.

Hennekam, R. C., Biesecker, L. G., Allanson, J. E., Hall, J. G., Opitz, J. M., Temple, I. K., & Carey, J. C. (2013). Elements of morphology: general terms for congenital anomalies. *American Journal of Medical Genetics Part A*, **161**(11), 2726-2733.

Formatted: Font: Italic

Formatted: Font: Bold

Holm, J. C., Refstie, T., & Bø, S. (1990). The effect of fish density and feeding regimes on individual growth rate and mortality in rainbow trout (*Oncorhynchus mykiss*). *Aquaculture*, **89**(3-4), 225-232.

Huysseune, A. (1995). Phenotypic plasticity in the lower pharyngeal jaw dentition of *Astatoreochromis alluaudi* (Teleostei: Cichlidae). *Archives of Oral Biology*, **40**(11), 1005-1014.

Huysseune, A., Sire, J. Y., & Meunier, F. J. (1994). Comparative study of lower pharyngeal jaw structure in two phenotypes of *Astatoreochromis alluaudi* (Teleostei: Cichlidae). *Journal of Morphology*, **221**(1), 25-43.

Kihara, M., Ogata, S., Kawano, N., Kubota, I., & Yamaguchi, R. (2002). Lordosis induction in juvenile red sea bream, *Pagrus major*, by high swimming activity. *Aquaculture*, **212**(1-4), 149-158.

Klingenberg, C. P. (2019). Phenotypic plasticity, developmental instability, and robustness: The concepts and how they are connected. *Frontiers in Ecology and Evolution*, **7**, 56. <https://doi.org/10.3389/fevo.2019.00056>

Koumoundouros, G., Gagliardi, F., Divanach, P., Boglione, C., Cataudella, S., & Kentouri, M. (1997). Normal and abnormal

885 osteological development of caudal fin in *Sparus aurata* L. fry.
886 *Aquaculture*, **149**(3-4), 215-226.

887 Kranenborg, S., Waarsing, J., Muller, M., Weinans, H., & van
888 Leeuwen, J. (2005). Lordotic vertebrae in sea bass (*Dicentrarchus*
889 *labrax* L.) are adapted to increased loads. *Journal of*
890 *Biomechanics*, **38**(6), 1239–1246.

891 Laerm, J. (1979). On the origin of rhipidistian vertebrae. *Journal of*
892 *Paleontology*, 175-186.

Formatted: Font: Italic

893 Lawrence, C. (2007). The husbandry of zebrafish (*Danio rerio*): a
894 review. *Aquaculture*, **269**(1-4), 1-20.

895 Lawrence, C., & Mason, T. (2012). Zebrafish housing systems: a
896 review of basic operating principles and considerations for design
897 and functionality. *ILAR journal*, **53**(2), 179-191.

898 Liew, W. C., Bartfai, R., Lim, Z., Sreenivasan, R., Siegfried, K. R., &
899 Orban, L. (2012). Polygenic sex determination system in zebrafish.
900 *PloS* *One*, **7**(4), e34397.
901 <https://doi.org/10.1371/journal.pone.0034397>.

902 Lisková, M., & Hert, J. (1971). Reaction of bone to mechanical
903 stimuli. 2. Periosteal and endosteal reaction of tibial diaphysis in
904 rabbit to intermittent loading. *Folia Morphologica*, **19**(3), 301–317.

905 Lleras Forero, L., Narayanan, R., Huitema, L. F. A., Vanbergen, M.,
906 Apschner, A., Peterson-Maduro, J., Logister, I., Valentin, G.,
907 Morelli, L.G., Oates, A.C., & Schulte-Merker, S. (2018).
908 Segmentation of the zebrafish axial skeleton relies on notochord
909 sheath cells and not on the segmentation clock. *ELife*, **7**, 1–28.

- 910 Matthews, M., Trevarrow, B., & Matthews, J. (2002). A virtual tour of
911 the guide for zebrafish users. *Resource*, **31**, 34-40.
- 912 Meyer, A. (1987). Phenotypic plasticity and heterochrony in
913 *Cichlasoma managuense* (Pisces, Cichlidae) and their implications
914 for speciation in cichlid fishes. *Evolution*, **41**(6), 1357-1369.
- 915 Nybelin, O. V. (1963). Zur morphologie und terminologie des
916 schwanzskelettes der Actinopterygier. *Arkiv för Zoologi*, **15**(35),
917 485-516.
- 918 Parichy, D. M., Elizondo, M. R., Mills, M. G., Gordon, T. N., &
919 Engeszer, R. E. (2009). Normal table of postembryonic zebrafish
920 development: Staging by externally visible anatomy of the living
921 fish. *Developmental Dynamics*, **238**(12), 2975–3015.
- 922 Pigliucci, M., Murren, C. J., & Schlichting, C. D. (2006). Phenotypic
923 plasticity and evolution by genetic assimilation. *The Journal of*
924 *experimental biology*, **209**(Pt 12).
925 <https://doi.org/10.1242/jeb.02070>.
- 926 Prestinicola, L., Boglione, C., Makridis, P., Spanò, A., Rimatori, V.,
927 Palamara, E., Scardi, M., & Cataudella, S. (2013). Environmental
928 Conditioning of Skeletal Anomalies Typology and Frequency in
929 Gilthead Seabream (*Sparus aurata* L., 1758) Juveniles. *PLoS*
930 *ONE*, **8**(2), e55736, <https://doi.org/10.1371/journal.pone.0055736>.
- 931 Ramsay, J. M., Feist, G. W., Varga, Z. M., Westerfield, M., Kent, M.
932 L., & Schreck, C. B. (2006). Whole-body cortisol is an indicator of
933 crowding stress in adult zebrafish, *Danio rerio*. *Aquaculture*,
934 **258**(1-4), 565-574.

- 935 Ribas, L., Valdivieso, A., Díaz, N., & Piferrer, F. (2017). Appropriate
936 rearing density in domesticated zebrafish to avoid masculinization:
937 links with the stress response. *Journal of Experimental Biology*,
938 **220**(6), 1056-1064.
- 939 Roo, J., Socorro, J., & Izquierdo, M. S. (2010). Effect of rearing
940 techniques on skeletal deformities and osteological development
941 in red porgy *Pagrus pagrus* (Linnaeus, 1758) larvae. *Journal of*
942 *Applied Ichthyology*, **26**(2), 372-376.
- 943 Roux W. (1881). Der züchtende Kampf der Teile, oder die
944 "Teilauslee" im Organismus (Theorie der "funktionellen
945 Anpassung"). Leipzig: Wilhelm Engelmann.
- 946 Rubin, C. T., & McLeod, K. J. (1994). Promotion of bony ingrowth by
947 frequency-specific, low-amplitude mechanical strain. *Clinical*
948 *Orthopaedics and Related Research*, **298**, 165–174.
- 949 Ruff, C., Holt, B., & Trinkaus, E. (2006). Who's afraid of the big bad
950 Wolff?: "Wolff's law" and bone functional adaptation. *American*
951 *Journal of Physical Anthropology: The Official Publication of the*
952 *American Association of Physical Anthropologists*, **129**(4), 484-
953 498.
- 954 Sæle, Ø., & Pittman, K. A. (2010). Looking closer at the determining
955 of a phenotype? Compare by stages or size, not age. *Journal of*
956 *Applied Ichthyology*, **26**(2), 294-297.
- 957 Schmalhausen, I. I. (1949).
958 Factors of evolution. (Transl. by I Dordick.) Philadelphia.
- 959 Schindelin, J., Arganda-Carreras, I., Frise, E., Kaynig, V., Longair,
960 M., Pietzsch, T., Preibisch, S., Rueden, C., Saalfeld, S., Schmid,
B., Tinevez, J-Y., White, D. J., Hartenstein, V., Eliceiri, K.,

961 Tomancak, P., & Cardona, A. (2012), "Fiji: an open-source
962 platform for biological-image analysis", *Nature methods*, **9**(7): 676-
963 682

964 Schmalhausen, I. I. (1949). *Factors of evolution*. (Transl. by I
965 Dordick.) Philadelphia.

966 Sfakianakis, D. G., Leris, I., Laggis, A., & Kentouri, M. (2011). The
967 effect of rearing temperature on body shape and meristic
968 characters in zebrafish (*Danio rerio*) juveniles. *Environmental
969 Biology of Fishes*, **92**(2), 197–205.

970 Shadwick, R. E., & Lauder, G. V. (Eds.). (2006). *Fish physiology:
971 Fish biomechanics* (Vol. 23). Elsevier.

972 Shelton, D. S., Price, B. C., Ocasio, K. M., & Martins, E. P. (2015).
973 Density and group size influence shoal cohesion, but not
974 coordination in zebrafish (*Danio rerio*). *Journal of Comparative
975 Psychology*, **129**(1), ~~72-77~~.

976 Slijper, E. J. (1942). Biologic anatomical investigations on the bipedal
977 gait and upright posture in mammals-With special reference to a
978 little goat born without forelegs II. *Proceedings of the Koninklijke
979 Nederlandse Akademie Van Wetenschappen*, **45**(1/5), 407-415.

980 Spoorendonk, K. M., Peterson-Maduro, J., Renn, J., Trowe, T.,
981 Kranenbarg, S., Winkler, C., & Schulte-Merker, S. (2008). Retinoic
982 acid and Cyp26b1 are critical regulators of osteogenesis in the
983 axial skeleton. *Development*, **135**(22), 3765-~~LP~~—3774.
984 <https://doi.org/10.1242/dev.024034>

985 Suniaga, S., Rolvien, T., Vom Scheidt, A., Fiedler, I. A. K., Bale, H.
986 A., Huysseune, A., Witten, P.E., Amling, M., & Busse, B. (2018).

Formatted: Not Highlight

987 Increased mechanical loading through controlled swimming
988 exercise induces bone formation and mineralization in adult
989 zebrafish. *Scientific Reports*, **8**(1), 1–13.

990 Taylor, W. R., & Van Dyke, G. C. (1985). Revised procedures for
991 staining and clearing small fishes and other vertebrates for bone
992 and cartilage study. *Cybium*, **9**, 107-119

993 Tibile, R. M., Sawant, P. B., Chadha, N. K., Lakra, W. S., Prakash,
994 C., Swain, S., & Bhagwati, K. (2016). Effect of stocking density
995 on growth, size variation, condition index and survival of discus,
996 *Symphysodon aequifasciatus* Pellegrin, 1904. *Turkish Journal of*
997 *Fisheries and Aquatic Sciences*, **16**(2), 453-460.

998 Tsang, B., Zahid, H., Ansari, R., Lee, R. C. Y., Partap, A., & Gerlai,
999 R. (2017). Breeding zebrafish: a review of different methods and a
1000 discussion on standardization. *Zebrafish*, **14**(6), 561-573.

1001 Turner, C H, Forwood, M. R., & Otter, M. W. (1994a).
1002 Mechanotransduction in bone: do bone cells act as sensors of fluid
1003 flow? *The FASEB Journal*, **8**(11), 875–878.

1004 Turner, C. H. (1998). Three rules for bone adaptation to mechanical
1005 stimuli. *Bone*, **23**(5), 399–407.

1006 Turner, C. H., Owan, I., & Takano, Y. (1995). Mechanotransduction
1007 in bone: role of strain rate. *American Journal of Physiology-*
1008 *Endocrinology and Metabolism*, **269**(3), E438–E442.

1009 Turner, Charles H., Forwood, M. R., Rho, J.-Y., & Yoshikawa, T.
1010 (1994b). Mechanical loading thresholds for lamellar and woven
1011 bone formation. *Journal of Bone and Mineral Research*, **9**(1), 87–
1012 97.

1013 van der Meulen, T. (2005). *Epigenetics of the locomotory system in*
1014 *zebrafish*. (Doctoral thesis, Wageningen University, The
1015 Netherlands). Retrieved from

<https://library.wur.nl/WebQuery/wurpubs/fulltext/121740>

1016 van Eeden, F. J. M., Granato, M., Schach, U., Brand, M., Furutani-
1017 Seiki, M., Haffter, P., Hammerschmidt, M., Heisenberg, C. P.,
1018 Jiang, Y. J., Kane, D. A., Kelsh, R. N., Mullins, M. C., Odenthal,
1019 J., Warga, R. M., Nüsslein-Volhard, C. (1996). Genetic analysis of
1020 fin formation in the zebrafish, *Danio rerio*. *Development*, **123**, 255-
1021 262.

Formatted: Font: Italic

Formatted: Font: Italic

Formatted: Font: Bold

1023 Waddington, C. H. (1953). Genetic assimilation of an acquired
1024 character. *Evolution*, **7**(2), 118-126.

1025 Wakeling, J. M., & Johnston, I. A. (1999). Body bending during fast-
1026 starts in fish can be explained in terms of muscle torque and
1027 hydrodynamic resistance. *The Journal of Experimental Biology*,
1028 **202**(1), 675–682.

1029 Wargelius, A., Fjellidal, P. G., & Hansen, T. (2005). Heat shock during
1030 early somitogenesis induces caudal vertebral column defects in
1031 Atlantic salmon (*Salmo salar*). *Development genes and*
1032 *evolution*, **215**(7), 350-357.

Formatted: Not Highlight

Formatted: Font: Italic, Not Highlight

Formatted: Not Highlight

1033 Weinans, H., & Prendergast, P. J. (1996). Tissue adaptation as a
1034 dynamical process far from equilibrium. *Bone*, **19**(2), 143-149.

1035 West-Eberhard, M. J. (2003). *Developmental plasticity and evolution*.
1036 Oxford University Press.

1037 West-Eberhard, M. J. (2005). Phenotypic accommodation: adaptive
1038 innovation due to developmental plasticity. *Journal of*

1039 *Experimental Zoology Part B: Molecular and Developmental*
1040 *Evolution*, **304**(6), 610-618.

1041 Westerfield, M. (2000). *The zebrafish book: a guide for the laboratory*
1042 *use of zebrafish*. 4th Edition, University of Oregon Press, Eugene

1043 Witten, P. E., & Hall, B. K. (2015). Teleost skeletal plasticity:
1044 modulation, adaptation, and remodelling. *Copeia*, **103**(4), 727-739.

1045 Witten, P. E., Gil-Martens, L., Hall, B. K., Huisseune, A., & Obach, A.
1046 (2005). Compressed vertebrae in Atlantic salmon *Salmo salar*:
1047 evidence for metaplastic chondrogenesis as a skeletogenic
1048 response late in ontogeny. *Diseases of aquatic organisms*, **64**(3),
1049 237-246.

1050 Witten, P. E., Obach, A., Huisseune, A., & Baeverfjord, G. (2006).
1051 Vertebrae fusion in Atlantic salmon (*Salmo salar*): Development,
1052 aggravation and pathways of containment. *Aquaculture*, **258**(1-4),
1053 164-172.

1054 Witten, P. E., Harris, M. P., Huisseune, A., & Winkler, C. (2017).
1055 Small teleost fish provide new insights into human skeletal
1056 diseases. In *Methods in cell biology* (Vol. 138, pp. 321-346).
1057 Academic Press.

1058 Witten, P. E., Huisseune, A., & Hall, B. K. (2010). A practical
1059 approach for the identification of the many cartilaginous tissues in
1060 teleost fish. *Journal of Applied Ichthyology*, **26**(2), 257-262.

1061 Witten, P. E., Obach, A., Huisseune, A., & Baeverfjord, G. (2006).
1062 Vertebrae fusion in Atlantic salmon (*Salmo salar*): development,
1063 aggravation and pathways of containment. *Aquaculture*, **258**(1-4),
1064 164-172.

- 1065 Wolff, J. (1892). *The law of bone transformation*. Berlin: Hirschwald.
- 1066 Wopat, S., Bagwell, J., Sumigray, K. D., Dickson, A. L., Huitema, L.
1067 F. A., Poss, K. D., Schulte-Merker, S., & Bagnat, M. (2018). Spine
1068 Patterning Is Guided by Segmentation of the Notochord Sheath.
1069 *Cell Reports*, **22**(8), 2094–2106.
- 1070 Ytteborg, E., Torgersen, J., Baeverfjord, G., & Takle, H. (2010).
1071 Morphological and molecular characterization of developing
1072 vertebral fusions using a teleost model. *BMC physiology*, **10**(1),
1073 **13**. <https://doi.org/10.1186/1472-6793-10-13>.
- 1074 Zouiten, D., Ben Khemis, I., Slaheddin Masmoudi, A., Huelvan, C., &
1075 Cahu, C. (2011). Comparison of growth, digestive system
1076 maturation and skeletal development in sea bass larvae reared in
1077 an intensive or a mesocosm system. *Aquaculture Research*,
1078 **42**(11), 1723–1736.

18
19
20
21
22
23
24
25
26
27
28
29
30
31
32
33
34
35
36
37
38
39
40
41
42

Abstract

The teleost zebrafish (*Danio rerio*), an established model for human skeletal diseases, is reared under controlled conditions with defined parameters for temperature and photoperiod. Studies aimed at defining the proper rearing density have been performed with regard to behavioural and physiological stress response, sex ratio and reproduction. Studies concerning the effect of rearing density on the skeletal phenotype are lacking. This study is designed to analyse the response of the skeleton to different rearing densities and provides a description of the skeletal deformities. Wild type zebrafish were reared up to 30 dpf (days post-fertilization) in a common environment. From 30 to 90 dpf, animals were reared at three different densities: high density (HD) 32 fish/L, medium density (MD) 8 fish/L and low density (LD) 2 fish/L. Animals at 30 and 90 dpf were collected and whole-mount stained with Alizarin red S to visualise mineralized tissues. The entire skeleton was analysed for meristic counts and 172 types of deformities. The results showed that rearing density significantly influenced the specimens' average standard length, which decreased with increasing rearing density. Differences concerning meristic counts among the three groups were not observed. Rearing density-independent malformations affected the ribs, neural arches and the spines of the abdominal region as well as vertebrae of the caudal complex. The HD group showed the highest number of deformities per specimens, the highest number of observed types of deformities and, together with the MD group, the

43 highest frequency of specimens affected by severe deformities. In
44 particular, the HD group showed deformities affecting arches, spines
45 and vertebral centra in the caudal region of the vertebral column.
46 This study provides evidence of an effect of rearing density on the
47 development of different skeletal phenotypes.

48 Keywords: deformities, plasticity, rearing density, skeleton, zebrafish

49

50
51
52
53
54
55
56
57
58
59
60
61
62
63
64
65
66
67
68
69
70
71
72
73
74

Introduction

Phenotypic plasticity, a component of phenotypic variation (Klingenberg, 2019), is the ability of living organisms to respond to environmental or internal stimuli through changes in behaviour, morphology or physiology, producing different phenotypes. Phenotypic plasticity can be adaptive or non-adaptive, reversible or irreversible, and its type and degree are specific to the single trait and the environmental conditions involved. In an evolutionary perspective, phenotypic plasticity is a feature of the reaction norm of a trait of single organisms (i.e. the complete set of phenotypic responses of a trait to a specific environmental variable), that can be the target of natural selection, steering towards phenotypic accommodation and genetic assimilation (Pigliucci et al., 2006, Schmalhausen, 1949, Waddington, 1953; West-Eberhard, 2003, 2005).

Phenotypic plasticity is particularly relevant for skeletal tissues. The vertebrate skeleton is composed of five main different skeletal tissue types: notochord, cartilage, bone, dentin and enamel/enameloid. In teleosts, several intermediate tissue types are present and skeletal tissues are considered part of a continuum (Hall and Witten, 2019; Witten et al., 2010). They are able to respond to intrinsic and extrinsic cues (Roux, 1881; Ruff et al., 2006; Weinans and Prendergast, 1996; Wolff, 1892). Skeletal tissues and cells are plastic and dynamic throughout life as they modulate their structure in response to the mechanical load regime. The processes through

75 which the skeletal cells achieve modifications are modulation,
76 metaplasia, transdifferentiation and remodelling (Hall and Witten,
77 2007; Witten and Hall, 2015). The ability of tissues to modulate their
78 phenotype in response to mechanical load is known as "Wolff's law
79 of bone transformation" (Wolff, 1892) or as "bone functional
80 adaptation" (Ruff et al., 2006). A famous example is the two-legged
81 goat, whose hind limbs and thoracic skeleton became modified to
82 adapt to the bipedal gait (Slijper, 1942).

83 Examples of phenotypic plasticity of the teleost skeleton are
84 numerous. In cichlids, differences in the hardness or type of food
85 modify the jaw shape, the number and strength of jaw bone
86 trabeculae and the size of replacement teeth (Huysseune, 1994,
87 1995; Meyer, 1987). The mechanical load exerted by swimming
88 changes the shape of vertebral centra and can induce lordosis in
89 different teleost species (Kihara et al., 2002; Kranenbarg et al.,
90 2005). Forced swimming accelerates ossification rate of vertebral
91 bodies and cartilage formation in the head and the caudal fin in
92 zebrafish *Danio rerio* (Hamilton 1822) (Fiaz et al., 2012; Suniaga et
93 al., 2018; van der Meulen, 2005).

94 The rearing of fish implies the modification and control of several
95 environmental factors (e.g., photoperiod, temperature, type of diet,
96 diet composition, hydrodynamics) in order to optimize rearing
97 conditions in aquaculture or laboratory facilities. Aquaculture-related
98 research provides numerous examples of how modifications of
99 environmental conditions change the skeletal phenotype, including
100 the induction of skeletal deformities.

101 In aquaculture, farming practices can be classified as intensive,
102 semi-intensive and extensive methodologies. They stand out for
103 several parameters, such as rearing density and tank volume,
104 hydrodynamics and diet. In intensive farming practice, rearing density
105 is high and tank volume smaller compared to semi-intensive and
106 extensive rearing conditions. The latter, besides being characterized
107 by decreased number of animal per volume and larger tanks, utilises
108 practises aimed at simulating the natural environment. This includes
109 differentiated hydrodynamics, and large live prey availability and
110 variety (Baluyut and Balnyme, 1995; Cataudella and Bronzi, 2001).
111 The above-mentioned rearing methodologies can affect the
112 morphology of the skeleton. In rainbow trout *Oncorhynchus mykiss*
113 (Walbaum 1792), the occurrence of skeletal deformities increases
114 significantly in animals reared in intensive conditions compared to
115 animals reared in extensive conditions (Boglione et al., 2014). Similar
116 observations have been reported for advanced marine teleosts:
117 gilthead seabream (*Sparus aurata* L.) and red porgy (*Pagrus pagrus*
118 L.) reared in semi-intensive conditions showed a lower number of
119 skeletal deformities per individual and a lower number of deformed
120 individuals (Prestinicola et al., 2013; Roo et al., 2010). Dusky grouper
121 (*Epinephelus marginatus* Lowe 1834) larvae reared in high-density
122 conditions showed the highest frequency of deformed individuals, the
123 highest number of deformities per deformed individual, the largest
124 range of types of deformities and the highest incidence of individuals
125 with at least one severe deformity (Boglione et al., 2009).

126 *Danio rerio* is an established model organism in biological and
127 biomedical research and is now also used as a model for human
128 skeletal diseases. Insights into fundamental pathways of skeletal
129 formation and skeletal diseases can be obtained, provided the
130 differences between the teleost and mammalian skeleton are
131 considered (Witten et al., 2017). Laboratory zebrafish are reared
132 under controlled conditions, with defined parameters for temperature
133 and photoperiod, but recommendations for rearing densities differ
134 (Castranova et al., 2011) and standards based on experimental data
135 are lacking (Lawrence and Mason, 2012). The Zebrafish Book
136 (Westerfield, 2000) recommends a rearing density of 0.55 adult
137 fish/L, whereas the “Guide for the care and use of laboratory
138 animals” (Clark et al., 1997) and Matthews et al. (2002) recommend
139 5 to 10 individuals/L for adult fish. Another published housing density
140 is 3.5 fish/L (Tsang et al., 2017). Concerning rearing densities for
141 early life stages, published data range from 6.5, up to 94 fish/L
142 (Carvalho et al., 2006; Goolish et al., 1998; Matthews et al., 2002).
143 As Lawrence (2007) emphasized, “the classifications of densities in
144 zebrafish research tend to vary considerably depending on the
145 experimental setting”. Remarkably, studies about the effects of the
146 rearing density in *D. rerio* are scarce (Ribas et al., 2017). Published
147 data refer to the animals’ sex ratio (Liew et al., 2012; Ribas et al.,
148 2017), growth rate (Hazlerigg et al., 2012; Ribas et al., 2017), stress
149 and behavioural parameters (Ramsay et al., 2006; Shelton et al.,
150 2015) or reproductive rates (Goolish et al., 1998). The effect of
151 rearing densities on the skeleton and the onset of skeletal deformities

152 in this species has not been reported. The skeletal phenotype of
153 transgenic and mutant zebrafish lines for genes related to human
154 skeletal pathologies has already been extensively described (Fisher
155 et al., 2003; Gray et al., 2014; Gistelinck et al., 2016; Haller et al.,
156 2018; Lleras Forero et al., 2018; Spoorendonk et al., 2008; Wopat et
157 al., 2018). Conversely, to our knowledge, the only works describing
158 the skeletal anomalies in wild type zebrafish are the study of age-
159 related deformities of Hayes et al. (2013) and a comprehensive
160 description of wild adult breeders and F1 juveniles *D. rerio* made by
161 Ferreri et al. (2000). The latter characterized 25 types of anomalies
162 affecting the vertebral column, vertebrae, fins and cranium.

163 The aim of this study was to analyse the response of the skeleton of
164 juvenile *D. rerio* to a single environmental variable, *i.e.* rearing
165 density. This study provides a description of skeletal deformities
166 developed in *D. rerio* reared at three different densities during the
167 juvenile stage.

168 **Materials and methods**

169 *Ethics statement*

170 All experiments were carried out at the Experimental Biology and
171 Aquaculture Laboratory, Università degli Studi di Roma Tor Vergata,
172 approved by the Animal-Welfare body and carried out in accordance
173 with Italian and European rules. All the animal experiments were
174 ethically approved and authorised by the General Director of the
175 Ministry of Health, Legislative Decree no.26/2014; European
176 Directive 2010/63/UE.

177 *Specimens maintenance and collection*

178 All the specimens used in this study were obtained from the same
179 pool of AB line (commonly referred to as wild type, WT) zebrafish
180 breeders (n= 15), male:female ratio 1:2, housed in a 25 L aquarium
181 equipped with a bio-mechanical filter. Eggs were obtained by natural
182 spawning. Vital eggs were incubated at 28°C until hatching. After
183 hatching, the animals were transferred in one large aquarium at a
184 density of 20 animals/L and maintained there up to 30 days post-
185 fertilization (hereafter, dpf), a time point when a stable number of
186 individuals was achieved (Figure_1_SupplInfo). At 30 dpf, the
187 specimens were randomly divided into groups and reared at three
188 densities: i) high (32 fish/L), ii) medium (8 fish/L) and iii) low density
189 (2 fish/L) (hereafter referred to as HD, MD and LD, respectively). The
190 choice was based on the need to find a compromise between having
191 a sufficient number of fish for the analyses (especially for the MD and
192 LD group) and the rearing densities adopted usually in the zebrafish
193 facilities (5 fish/L for the adult stage). The remaining fish were
194 euthanized with a lethal dose (500 µl/L) of 2-phenoxyethanol and
195 fixed (1.5% glutaraldehyde and 1.5% paraformaldehyde in 0.1 M
196 cacodylate buffer, pH 7.4) representing a “time zero” sampling point
197 (hereafter referred to as T0).

198 The water used for all the tanks (breeders, eggs, larvae and
199 juveniles) was obtained mixing equal parts of water treated by
200 reverse osmosis water and 50 µm-filtered well water. The
201 photoperiod was 14L:10D and water parameters were maintained as

202 follows: water temperature 28°C, pH 6.8-8.5, water hardness 60-200
203 mg/L CaCO₃, nitrite and ammonia 0 mg/L, nitrate < 50 mg/L. Fish
204 were fed twice per day *ad libitum* with *Artemia salina* (L.) nauplii and
205 dry commercial food of different size according to the developmental
206 stages (Micron, Sera; Tetramin Baby, Junior and Flakes, Tetra®).

207 *Experimental system and samples collection*

208 The experimental rearing based on the three different density groups
209 lasted 60 days, from 30 to 90 dpf. The experimental rearing at the
210 three densities was carried out in a recirculating housing system
211 composed of nine interconnected 3.5 L trapezoidal tanks, equipped
212 with a mechanical/biological filter, air and water pumps. Water
213 exchange was 400 ml/min. Temperature, photoperiod and water
214 parameters were the same as reported above.

215 At the end of the experimental rearing, fish were euthanized and
216 fixed (as above). After 48 hours of fixation at 4°C, all the samples
217 were dehydrated in a graded ethanol series and stored in 70%
218 ethanol at 4°C until the analyses were performed.

219 The number of specimens used for the analyses was T0, n=32; HD,
220 n=65; MD, n=46 and LD, n=19.

221 *Staining*

222 Specimens were whole-mount stained for mineralized tissues with
223 Alizarin red S (modified from Taylor and Van Dyke, 1985). Samples
224 were first rehydrated in a graded ethanol series, washed in distilled
225 water and bleached with a 0.45% H₂O₂ and 0.5% KOH solution until

226 the depigmentation was achieved, rinsed in distilled water and
227 transferred in saturated borax for 24h. Samples were then stained
228 with 0.01% Alizarin red S in 0.5% KOH overnight or longer, according
229 to the specimen's size, rinsed in distilled water, placed in 1% KOH for
230 2h, finally cleared and dehydrated in a graded series of KOH-glycerol
231 solutions and stored in 100% glycerol. The standard length (S_L , mm)
232 of individuals was then measured on digital images using the
233 software Fiji (Schindelin et al., 2012). Individuals were analysed for
234 meristic counts and skeletal anomalies using a Zeiss Axio Zoom V16
235 Stereo Zoom Microscope equipped with a 5MP CCD camera.

236 *Meristic counts and analyses of skeletal anomalies*

237 Meristic counts were carried out on the number of vertebrae of each
238 region of the vertebral column, fin rays of unpaired and paired (left
239 and right side) fins and their inner supports, and supraneural bones.
240 Nomenclature for skeletal elements follows Arratia et al. (2001) and
241 De Clercq et al. (2017). The vertebral column was subdivided into
242 four different regions, with nomenclature adapted from Bensimon-
243 Brito et al. (2012a). These authors combined the terminologies of
244 Arratia et al. (2001), Bird and Mabee (2003) and Nybelin (1963) as
245 follows: 1) Weberian region (vertebrae bearing the Weberian
246 ossicles), 2) abdominal region (rib-bearing vertebrae with open
247 haemal arches), 3) caudal region (vertebrae with closed haemal
248 arches) and 4) caudal complex (preurals and ural vertebrae with
249 modified haemal and neural arches and spines).

250 The use of the terms “anomaly”, “malformation” and “deformity”
251 follows Boglione et al. (2013) and Hennekam et al. (2013).
252 Malformations are early developmental defects; deformities are
253 defects that relate to later, epigenetic, factors. We reserve the use of
254 the term anomaly for the description of the methodology adopted in
255 this study and the cases for which nor “malformation” and
256 “deformation” can be used. Skeletal anomalies were classified using
257 an alphanumeric code (modified from Prestinicola et al., 2013),
258 where the capital letter indicates the affected skeletal region, the
259 numbers refer to the skeletal elements and the lowercase letters to
260 the types of anomalies (Table 1).

261 For each group (T0, HD, MD and LD), the following general metrics
262 were calculated: 1) frequency (%) of individuals with at least one
263 anomaly; 2) number of types of anomaly observed; 3) average
264 anomaly load (total number of anomalies recorded in a group/number
265 of malformed individuals per group); 4) frequency (%) of individuals
266 with at least one severe anomaly; 5) frequency (%) of observed
267 severe anomalies on the total number of observed anomalies; 6)
268 average severe anomaly load (number of severe anomalies/number
269 of individuals with severe anomalies); 7) frequency (%) of each type
270 of anomaly, with respect to the total number of anomalies observed
271 in each group. In this paper, severe anomalies refer to those types of
272 anomalies that affect the vertebral axis (*i.e.*, scoliosis, lordosis,
273 kyphosis) and centra (deformation, elongation and reduction in
274 length, and fusion).

275 The phenotypic analysis of the skeleton was carried out based on
276 certain assumptions (adapted from Prestinicola et al., 2013): i) non-
277 completely fused vertebral centra were counted as distinct elements
278 in meristic counts while those completely fused as one; ii)
279 supernumerary bones with normal morphology were not considered
280 as anomalies but included as meristic count variations; conversely,
281 anomalous supernumerary elements were included among
282 anomalies; iii) upon simple visual inspection, only the identifiable
283 deformations in shape were considered as skeletal anomalies: if any
284 doubts arose, then the shape variation was not considered
285 anomalous; iv) curvatures of the vertebral column were considered
286 as scoliosis, lordosis and/or kyphosis only if the involved vertebral
287 centra were deformed, in order to exclude from the analyses axis
288 deformations due to neuromuscular anomalies or fixation artefacts.

289 *Statistical analyses*

290 Data obtained for the S_L and vertebrae counts were compared with
291 the Kruskal-Wallis test followed by Dunn's *post-hoc* test with the
292 Bonferroni correction.

293 Data obtained from the analysis of skeletal anomalies were used to
294 build a *Raw Matrix* (hereafter referred to as RM). The RM was
295 transformed into a *Binary Matrix* (hereafter named BM: presence of
296 each type of skeletal malformation = 1; absence = 0). RM was used
297 to calculate the frequencies (%) of each type of anomaly on the total
298 number of anomalies. The BM was used to calculate the frequencies
299 (%) of individuals affected by each type of anomaly in each group.

300 The frequencies obtained from the RM and the BM are presented
301 with tables or histograms. Statistical differences among groups were
302 tested with one-way PERMANOVA (9999 permutations) using both
303 the RM (Euclidean distance) and the BM (simple-matching) matrices.
304 RM and BM, and other matrices built on a subset of data were
305 subjected to Correspondence Analysis (CA) (Benzécri et al., 1973) in
306 order to visualize the relationships among groups and the role that
307 each anomaly plays in defining the characteristics of the different
308 groups.

309 Statistics was performed with the software Past 3.20 (Hammer et al.,
310 2001).

311 **Results**

312 *T0 group*

313 The average SL of the T0 specimens was 7.6 (± 1.7 SD) mm. All
314 caudal fin elements were identifiable in each T0 specimen. The
315 modal value and the range values of the T0 vertebral centra
316 (calculated excluding the specimens with vertebral centra still
317 mineralizing) were 34 and 32-35, respectively (Table 2).

318 The general metrics for the T0 group are summarised in Table 3. The
319 frequency of specimens affected by at least one anomaly and at least
320 one severe anomaly was 56% and 34%, respectively. The average
321 anomaly load (average number of anomalies per malformed
322 specimen) and the average severe anomaly load (average number of
323 severe anomalies per malformed specimen) was 9 and 2,
324 respectively. The number of observed types of anomalies was 17

325 (see Figure 1). Severe anomalies represented 12% of all anomalies.
326 Severe anomalies were represented by centra deformation (type
327 2def and elo/red) and scoliosis (1sco). The frequencies (%) of each
328 type of anomaly on the total number of anomalies counted in the T0
329 group and the frequency of the specimens affected by each anomaly
330 are reported in Figure 1. The most common (22-41% of T0
331 specimens) malformations were those affecting the neural arches of
332 the abdominal region (B4def) and the ribs (B7def), scoliosis in
333 vertebrae of the caudal complex (D1sco) and malformations of the
334 epural (G11def). No lordosis, kyphosis, nor fusions of vertebral
335 centra were recorded in the T0 individuals (except for one partial
336 fusion in the caudal complex vertebrae, D2par, in one fish).

337 *Experimental groups (HD, MD and LD)*

338 S_L significantly differed among groups (Kruskal-Wallis: $H=38.9$,
339 $p<0.001$). Specifically, $LD>MD>HD$ ($p<0.01$ for each pairwise Dunn's
340 test) (Figure 2).

341 The data referring to the meristic counts are shown in Table 2. The
342 modal value of the number of vertebral centra (= 33) and the lower
343 limit of its range of variation (=30) were lower in the HD group than in
344 MD and LD group. This is due to the presence of specimens affected
345 by complete fusion of vertebral centra in the HD group, as reported
346 below.

347 Given that four types of malformation were commonly observed in
348 the T0 group (B4def, B7def, D1sco and G11def), these were
349 considered as "background malformations" for this zebrafish batch

350 when the experimental animals were analysed, and removed from
351 the analysis of the experimental groups. Indeed, they occurred at
352 similar percentages in specimens of all experimental groups.

353 The general metrics referring to the analysis of the skeletal
354 anomalies for each group are presented in Table 4. The frequency
355 (%) of specimens with at least one skeletal anomaly was 100 in the
356 HD and LD groups and 98 the MD group (*i.e.* one specimen in the
357 MD group was only affected by some of the above-mentioned
358 “background malformations”). The highest average anomaly load
359 was found in the HD group (12 anomalies/deformed specimen), as
360 well as the widest variety of observed types of anomalies (n=68). The
361 highest frequencies of specimens with at least one severe anomaly
362 (73%) as of severe anomalies relative to the total number of
363 anomalies (21.4%) were observed in the MD group.

364 Statistically significant differences were found between the HD and
365 the other two experimental groups (MD and LD) (PERMANOVA,
366 $p < 0.01$). The frequencies (%) of deformities grouped per skeletal
367 element and per region, and the frequency of affected specimens are
368 represented in Figure 3 (raw data are provided in the Table_1_
369 SuppInfo), for each experimental group.

370 None of the following deformities was found in any experimental
371 group: lordosis in the Weberian, abdominal or caudal complex
372 regions (A1lor, B1lor and D1lor), kyphosis (code 1kyp), partial fusion
373 in the Weberian and abdominal region (A2par and B2par), elongated
374 vertebral centrum of the abdominal, caudal and caudal complex
375 regions (B2elo, C2elo and D2elo), demineralization of the urostyle

376 (D3dec), deformities of fin elements such as coracoid (code 20),
377 post-cleithrum (code 21), pectoral radials (E8sup/abs), pelvic
378 pterygiophores (L8abs and def) and rays (I12abs), anal
379 pterygiophores (F8sup) and rays (F12abs and def), dorsal
380 pterygiophores (H8abs, fus and dec) and rays (H12abs), epural
381 (G11sup) and caudal rays (G12sup), and cranial deformities such as
382 maxilla/premaxilla deformation (code 13), deformations of the
383 opercula (code 16) or branchiostegal rays (17sup, abs and def L),
384 neurocranium deformities (15) and saddle-back syndrome (1sbs).

385 The Weberian (code A) and abdominal vertebral (code B) regions
386 were the least affected skeletal regions in all the experimental groups
387 (see Table_1_ SuppInfo), with the exception of neural arches in the
388 Weberian vertebrae (malformation A4def) and supraneurals (A18
389 and A18sup).

390 The HD and MD groups showed the highest frequency of deformities
391 (Figure 3a) and frequency of individuals with deformities (Figure 3b)
392 affecting centra (Cc) and centra-associated elements of the caudal
393 region (Cae). In particular, the HD group showed the highest
394 percentage of individuals with deformities in the caudal region
395 (Figure 3b), both for centra-associated elements (Cae) (almost all the
396 C4 types and C5def, Figure 4b) and centra (Cc) (C2fus and def,
397 Figure 4b). In the MD group, the highest frequency of deformities
398 (Figure 4a) of the caudal vertebral centra (in particular C2par) was
399 found. Lastly, pectoral and anal fins were more frequently deformed
400 in the HD group.

401 The LD group showed the highest frequency of neural arch
402 deformities affecting the Weberian vertebrae (Aae in Figure 3, A4def
403 in the Table_1_ SupplInfo) as well as the caudal fin elements (fin rays
404 and inner supports) (Figure 3). The LD group also displayed the
405 highest frequency of deformities affecting the centra of the caudal
406 complex, although the frequency of the specimens affected by these
407 deformities was higher in the MD group (Dc, Figure 3). Different from
408 HD and MD, some deformities were never present in the LD group,
409 *i.e.*, lordosis (C1lor), complete vertebral centra fusion (C2fus),
410 misplacement of the neural arch insertions (C4ins) and mismatched
411 fusion of neural and haemal spines (C4mis and C5mis), absence of
412 neural or haemal arches or spines (C4abs, C4abs R, C5abs) and
413 scoliosis (C1sco).

414 In Figure 5, examples of some of the deformities recorded are
415 provided.

416 *Correspondence Analysis (CA)*

417 Different CAs were performed on different matrices in order to
418 visualize the differences or relationships among samples and the role
419 each anomaly played in defining the characteristics of each group.
420 The CA applied to RM or BM, containing all the specimens and the
421 observed types of deformities (matrices 129 specimens x 86 types of
422 deformities). Note that one individual of the MD without any
423 deformities was not included in the matrix, since a null data vector,
424 *i.e.* a record for a specimen without anomalies, cannot be processed
425 by any of the techniques that require vector normalisation, e.g. by

426 correspondence analysis. The CA applied to RM and BM gave
427 ordination models exhibiting a very low variance for the first three
428 axes (14% and 13%, respectively). Therefore, they are not shown. CA
429 was next applied to a subset of data obtained from the RM containing
430 19 randomly sampled individuals per group. This number of samples
431 was chosen on the base of the sample size of the LD group, in order
432 to avoid bias due to differences in the sample's dimension. The final
433 matrix was 57 specimens x 12 descriptors. The CA explained an
434 overall variance of 55% for the first three axes of correspondences.
435 In Figure 6, the ordination model obtained on CA1 and CA2 axes
436 (explaining 43% of the variance) is shown for each group on different
437 graphs. The HD centroid plots on the 3rd quadrant (negative semi-
438 plane of CA1), where the deformities of the centra-associated
439 elements (Bae and Cae) and vertebral centra (Bc and Cc) of the
440 abdominal and caudal regions are located. The MD and LD centroids
441 are positioned in the positive half-space of CA 1, with MD in an
442 intermediate position with respect to HD and LD groups. Most
443 individuals of the MD and LD groups are located in the 1st quadrant,
444 overlapping with malformations of the associated elements of the
445 Weberian vertebrae and of the pectoral and caudal fins. In all groups,
446 only a few specimens of the three experimental groups were
447 positioned in the 4th quadrant, where deformities of the anal and
448 dorsal fins and associated elements of the caudal complex vertebrae
449 are situated.

450 **Discussion**

451 This paper describes the phenotypic plasticity of the skeleton and the
452 occurrence of skeletal deformities in wild-type *D. rerio* reared under
453 identical conditions, with rearing densities being the only variable.
454 Our results reveal (1) the presence of certain anomalies in zebrafish
455 of different age and experiencing different experimental conditions
456 (T0, HD, MD and LD), (2) a significant difference in size (S_L)
457 depending on rearing densities, and (3) a higher incidence of
458 deformities of vertebrae of the caudal region in animals reared at
459 higher densities, in particular deformities of arches and spines and
460 fusion of vertebral centra, discussed below.

461 *Rearing density-independent skeletal malformations: the starting*
462 *point (T0)*

463 Animals at the same age (30 dpf), but of different sizes (S_L), show
464 that skeletal development is more advanced in larger individuals
465 compared to smaller individuals. This confirms the findings in
466 previous studies that show a better correlation of skeletal
467 development with size than with age, in *D. rerio* (Cubbage and
468 Mabee, 1996; Parichy *et al.*, 2009) and in farmed fish, *i.e.* Atlantic
469 halibut (*Hippoglossus hippoglossus* L.) (Sæle and Pittman, 2010).

470 The analysis of the skeletal phenotype at the beginning of the
471 experiment allowed identifying malformations of the ribs (B7def), and
472 neural arches and spines in the abdominal region (B4def), scoliosis
473 in the caudal complex (D1sco) and malformations of the epural
474 (G11def) as “background malformations” for the zebrafish used in
475 this study. The presence of malformed ribs and neural arches of the

476 abdominal region reported in the present work is in agreement with
477 the study of Ferreri et al. (2000). In their work, reared specimens
478 displayed a higher frequency of individuals affected by the
479 aforementioned malformations than wild zebrafish sampled from the
480 river Ganges. Even in wild specimens, about 13% of ribs and 21% of
481 neural arches and spines (although not assigned to distinct regions)
482 were diagnosed as malformed. The high incidence of malformations
483 of neural arches and spines in the abdominal region (close to 100%
484 of the analysed specimens) and the presence of malformed ribs
485 (ranging from 39 to 80%) was also reported for *O. mykiss* reared
486 both at low and high densities (Boglione *et al.*, 2014). Thus, similar to
487 *O. mykiss*, *D. rerio* appears to be susceptible to develop these
488 particular malformations.

489 Other malformations were found to be present with low frequencies
490 in the T0 specimens, e.g., malformations of the caudal complex, *i.e.*
491 D1sco (22%), D3def (6%), D4def5 (13%), and D2def (13%).
492 Interestingly, no fusions were detected, except for a single
493 occurrence in the caudal complex (D2par). It is recognised that the
494 vertebrae of the caudal complex display a high degree of plasticity
495 and its predisposition to develop vertebral centra fusions is well
496 documented at least in some species (Bensimon-Brito et al., 2010,
497 2012b; Gavaia et al., 2002; Koumoundourous et al., 1997,
498 Prestinicola et al., 2013; Witten et al., 2006). As part of normal
499 development, the last vertebral body – the urostyle – in zebrafish
500 forms through five fusion events (Bensimon-Brito et al., 2010,
501 2012b). The preural vertebral centra, which frequently possess an

502 accessory arch, show a higher tendency to fuse than the vertebrae of
503 the anteriormost regions (Bensimon-Brito et al., 2012b; Eastman,
504 1980).

505 *Effects of the rearing densities*

506 Specimens reared at high density (HD) showed a significantly
507 reduced growth with respect to the specimens reared at medium and
508 low densities. An inverse relation between growth and rearing density
509 has also been described for zebrafish reared from 6 to 90 dpf at 19,
510 37 and 74 fish/L (Ribas et al., 2017), as well for other basal teleost
511 species such as *O. mykiss*, and for advanced teleosts such as *H.*
512 *hippoglossus* and discus (*Symphysodon aequifasciatus* Pellegrin
513 1904) (Björnsson, 1994; Holm et al., 1990; Tibile et al., 2016). It has
514 been proposed that size differences relate to the reduction in feeding
515 activity or to an increase in energy expenditure associated with
516 enhanced swimming activity due to increased competition or
517 interactions. In our experimental rearing, food was administered *ad*
518 *libitum*, consequently, insufficient feeding was unlikely a causative
519 factor for the reduced size in the specimens reared at higher
520 densities.

521 Rearing at different densities after 30 dpf did not influence the modal
522 values of meristic characters. Lower mean values and lower limit of
523 the variation range for the number of vertebral centra observed in the
524 HD reared zebrafish related to the presence of complete vertebral
525 centra fusions (which in the meristic counts were accounted as one
526 element). Ferreri et al. (2000) compared wild and reared zebrafish

527 and found similar ranges of variation for several meristic elements,
528 with the exception of the anal and pectoral fin rays. Bird and Mabee
529 (2003) confirmed what Ferreri et al. (2000) previously reported for
530 vertebral centra counts even in other reared zebrafish. Usually,
531 variation in the number of meristic elements is due to changes in
532 environmental conditions during the early developmental stages. For
533 example, low temperatures lead to an increased number of vertebrae
534 in reared zebrafish (Sfakianakis et al., 2011).

535 All the specimens analysed (with one exception in the MD group,
536 already discussed) showed at least one anomaly (Table 4). Such a
537 high frequency may be surprising but has been reported before. High
538 frequencies of zebrafish affected by at least one anomaly were
539 already reported for both wild (87%) and reared (93%) specimens by
540 Ferreri et al. (2000).

541 The HD group displayed the highest average number of deformities
542 per specimen and a larger variety of types of deformities. The latter
543 could be a density effect but it could also relate to the larger number
544 (n = 65) of HD specimens with respect to the MD (n = 46) and LD (n
545 = 19) groups. However, the highest average number of deformities
546 per specimen, as detected in the HD group, parallels what has been
547 already described in aquaculture facilities. Semi-intensive rearing
548 methodologies (characterized also by reduced rearing densities)
549 compared to intensive rearing conditions, decrease the occurrence of
550 skeletal deformities in farmed fish (Boglione et al., 2009; Prestinicola
551 et al., 2013; Zouiten et al., 2011). Similar to what has been described
552 for an advanced teleost, the *E. marginatus* (Boglione et al., 2009),

553 rearing density alone can affect the skeletal phenotype in zebrafish,
554 and increases the occurrence of particular types of deformities in the
555 caudal region of the vertebral column (partial and complete fusions of
556 vertebral centra, deformation of neural and haemal arches). The
557 susceptibility of the caudal region to deformities has been already
558 described in farmed Atlantic salmon (*Salmo salar* L.). Vertebral
559 centra compressions and fusions can relate to high-temperature
560 exposure during the embryonic stages (Grini et al., 2011). The
561 aggravation of such deformities in salmonids reared at high
562 temperature can occur later, for example during the late juvenile
563 seawater phase (Wargelius et al., 2015). The latter may be the result
564 of a synergic effect of the rearing temperature and the high density
565 used during the seawater rearing. Vertebral centra deformities in
566 Atlantic salmon have also been attributed to other not fully elucidated
567 causative factors acting during later ontogenetic stages (Fjellidal, et
568 al., 2007, Fjellidal et al., 2012).

569 The skeletal elements that displayed the most distinct phenotypic
570 response to increased rearing density were neural and haemal
571 arches and spines (deformations in shape, C4def and C5def),
572 followed by centra of the caudal region (C2par and fus). Despite the
573 fact that anomalies of arches and spines were also observed in a few
574 specimens of the T0 group, their frequency, and that of specimens
575 affected, are far higher in the HD than in the LD group. Vertebral
576 centra and arches in teleosts are different developmental modules.
577 Vertebral centra originate as chordacentra by mineralization of the
578 notochord sheath, whilst the associated elements arches and spines

579 are patterned by the somites (Laerm, 1979, Fleming et al., 2015).
580 The duality in vertebral column elements' formation could explain the
581 higher incidence of deformities of arches and spines compared to
582 vertebral centra, in the HD group. Interestingly, malformations,
583 similar to those shown in Fig. 5c, have been described for fused
584 somite mutant zebrafish (tbx6 mutation) (van Eedden et al., 2006,
585 Fleming et al., 2004). In this mutant zebrafish line, the somitogenesis
586 is disturbed and the specimens show malformations of arches and
587 spines, but separated vertebral centra. That shows that centra and
588 associate elements are two distinct developmental modules.
589 However, the mechanisms by which rearing density induces late
590 vertebral column deformities that resemble mutant-related
591 malformations remain to be elucidated. Deformities of arches and
592 spines have also been related to musculature impairments (Favaloro
593 et al., 2006, Backiel et al., 1984). Behavioural studies on *O. mykiss*
594 reared at high stocking densities (Bégout Anras and Lagardère,
595 2004; Cooke et al., 2000) showed that the complexity of swimming
596 trajectories, space utilization and activity rhythms were altered and
597 that swimming activity, oxygen consumption and muscular activity
598 increased when compared with individuals reared at lower densities.
599 Moreover, the crowded conditions augmented the occurrence of
600 changes in swimming direction with sharper turning angles with
601 respect to individuals kept at lower densities (Bégout Anras and
602 Lagardère, 2004). The swimming patterns suggested recurring
603 avoidance behaviours of individuals held in the same tank.
604 Avoidance behaviours imply the utilization of fast C-start movements,

605 usually occurring during escape responses, which start with the
606 contraction of the muscles of one side of the body, at the level of the
607 individual's centre of mass, in which the propulsive force develops,
608 allowing the fish to change orientation (Eaton and Emberley, 1991).
609 During the fast start movements, the body bends at the level of the
610 central region, below the dorsal fin, at the 50% of the fish T_L , as
611 shown for zebrafish by Danos and Lauder (2012). In *Cyprinus carpio*
612 the maximum vertebral column curvature has been calculated to be
613 between 50 and 80% of fish T_L (Shadwick and Lauder, 2006).
614 During fast start movements, the muscles generate a mechanical
615 load on the flexing vertebral column (Shadwick and Lauder, 2006;
616 Wakeling and Johnston, 1999).
617 Mechanical loading increases bone formation in zebrafish (Fiaz et al.,
618 2010; Suniaga et al., 2018) especially if its frequency is high and the
619 mechanical load is dynamic, rather than static (Lisková and Hert,
620 1971; Rubin and McLeod, 1994; Turner, 1998; Turner et al., 1994a,b;
621 Turner et al., 1995).
622 Therefore, if a crowded environment leads to an increased number of
623 interactions between animals and thus changes in swimming
624 trajectories, for example due to food competition, possibly, the centra
625 of the central region (*viz.* caudal) of animals reared at higher
626 densities are more often subjected to the bendings generated by the
627 axial musculature. The C-shaped bending of an elongated structure,
628 such as the vertebral column, produces compression on the concave
629 side and strain on convex one. Thus, the intervertebral space on the
630 concave side of the bending would be subjected to compression, i.e.

631 mechanical loading. Indeed, the concave and convex sides can
632 reverse from fast movement to another, according to the turning
633 direction. This increased elicitation could explain the occurrence of
634 fusion in the caudal region of the vertebral column.

635 In this study, the complete fusion of vertebral centra (C2fus) was
636 never observed in specimens reared at low density. Partial fusions
637 (C2par) occurred at a lower frequency in LD compared to the HD and
638 MD groups. Ferreri et al. (2000), using densities far lower than the
639 LD used in this work, did not record vertebral fusion, suggesting that
640 their occurrence and severity could be linked to the increased rearing
641 density. Vertebral centra fusion can develop at various time points
642 during development. Very early fusions in zebrafish relate to the
643 ectopic mineralisation of the notochord sheath in prospective
644 intervertebral regions (Bensimon-Brito et al., 2012b). It is unlikely that
645 this type of very early fusions accounts for observations made in this
646 experiment: notochord segmentation takes place during early
647 ontogeny and it would not explain differences in the occurrence of
648 vertebral fusions in animals reared at different rearing densities
649 during the juvenile period when the vertebral centra identity is
650 already determined. Further, animals from the T0 group did not show
651 fused vertebrae.

652 The next (early) process that can cause the fusion of vertebral centra
653 in zebrafish is the bridging of intervertebral spaces by bone that
654 develops around the mineralised notochord sheath (Bensimon-Brito
655 et al., 2012b; Ytteborg et al., 2010). A third process that may lead to
656 a late fusion (not described in zebrafish but in *S. salar*), is caused by

657 metaplasia, *i.e.* osteoblasts of the vertebral endplate growth zone
658 turn in cells with a chondroblast-like phenotype, producing cartilage
659 in the intervertebral space. This ectopic cartilage later mineralizes
660 and is subsequently remodelled into bone (Fjellidal et al., 2012;
661 Witten et al., 2005; 2006; Ytteborg et al., 2010).

662 In conclusion, our study shows the effect of rearing density on the
663 growth rate of zebrafish and provides evidence that rearing density
664 affects the skeletal phenotype in this species. High and, to some
665 extent, medium rearing densities slowed down growth and induced
666 deformities, particularly in the caudal region of the vertebral column.
667 Our results suggest that a density of 2 fish/litre, between the age of
668 30 and 90 dpf can help to reduce the incidence of skeletal
669 malformations in *D. rerio*. This is especially relevant if zebrafish is
670 used for studying skeletal pathologies. Moreover, for this analysis,
671 we propose a methodology that is adaptable and can be used in
672 various contexts to assess skeletal anomalies in zebrafish or other
673 species. For example, the alphanumeric code used here can be
674 adapted to different levels of details according to the needs or
675 applications (*i.e.*, by grouping different types of malformations, or by
676 adding subcodes for peculiar or different types of malformations).
677 Such standardization may facilitate comparison among different
678 studies.

679 **Acknowledgements:** We are grateful to A. Forlino for providing the
680 zebrafish breeders used in this study. This research is a part of the
681 Ph.D. thesis of Arianna Martini.

682 **Author contributions:** CB and PEW conceived the experimental
683 design, AM carried out the experiments, performed the analyses and
684 elaborated the data; AM, AH, PEW and CB discussed the results and
685 wrote the paper. All authors have approved the final version of the
686 manuscript.

687 **References**

688 Arratia, G., Schultze, H. P. & Casciotta, J. (2001). Vertebral column
689 and associated elements in dipnoans and comparison with other
690 fishes: development and homology. *Journal of Morphology*,
691 **250**(2), 101-172

692 Backiel, T., Kokurewicz, B., & Ogorzałek, A. (1984). High incidence
693 of skeletal anomalies in carp, *Cyprinus carpio*, reared in cages in
694 flowing water. *Aquaculture*, **43**(4), 369-380.

695 Baluyut, E. & Balnyme, E. (1995). *Aquaculture systems and*
696 *practices: a selected review*. Daya Books

697 Bégout Anras, M.L. & Lagardère, J. P. (2004). Measuring cultured
698 fish swimming behaviour: first results on rainbow trout using
699 acoustic telemetry in tanks. *Aquaculture*, **240**(1–4), 175–186.

700 Bensimon-Brito, A., Cancela, M. L., Huisseune, A., & Witten, P. E.
701 (2010). The zebrafish (*Danio rerio*) caudal complex - a model to
702 study vertebral body fusion. *Journal of Applied Ichthyology*, **26**(2),
703 235–238.

704 Bensimon-Brito, A., Carneira, J., Cancela, M. L., Huisseune, A., &
705 Witten, P. E. (2012a). Distinct patterns of notochord mineralization
706 in zebrafish coincide with the localization of Osteocalcin isoform 1

707 during early vertebral centra formation. *BMC Developmental*
708 *Biology*, **12**(28), <https://doi.org/10.1186/1471-213X-12-28>.

709 Bensimon-Brito, A., Cancela, M. L., Huysseune, A., & Witten, P. E.
710 (2012b). Vestiges, rudiments and fusion events: the zebrafish
711 caudal fin endoskeleton in an evo-devo perspective. *Evolution &*
712 *Development*, **14**(1), 116–127.

713 Benzécri, J. P. (1973). *L'analyse des données* (Vol. 2, p. I). Paris:
714 Dunod.

715 Bird, N. C., & Mabee, P. M. (2003). Developmental morphology of
716 the axial skeleton of the zebrafish, *Danio rerio* (Ostariophysi:
717 Cyprinidae). *Developmental dynamics*, **228**(3), 337-357.

718 Björnsson, B. (1994). Effects of stocking density on growth rate of
719 halibut (*Hippoglossus hippoglossus* L.) reared in large circular
720 tanks for three years. *Aquaculture*, **123**(3-4), 259-270.

721 Boglione, C., Marino, G., Giganti, M., Longobardi, A., De Marzi, P., &
722 Cataudella, S. (2009). Skeletal anomalies in dusky grouper
723 *Epinephelus marginatus* (Lowe 1834) juveniles reared with
724 different methodologies and larval densities. *Aquaculture*, **291**(1–
725 2), 48–60.

726 Boglione, C., Gisbert, E., Gavaia, P., Witten, P. E., Moren, M.,
727 Fontagné, S., & Koumoundouros, G. (2013). Skeletal anomalies in
728 reared European fish larvae and juveniles. Part 2: main typologies,
729 occurrences and causative factors. *Reviews in Aquaculture*, **5**,
730 S121-S167.

731 Boglione, C., Pulcini, D., Scardi, M., Palamara, E., Russo, T., &
732 Cataudella, S. (2014). Skeletal anomaly monitoring in rainbow

733 trout (*Oncorhynchus mykiss*, Walbaum 1792) reared under
734 different conditions. *PloS one*, **9**(5), e96983
735 <https://doi.org/10.1371/journal.pone.0111294>. Carvalho, A. P.,
736 Araújo, L., & Santos, M. M. (2006). Rearing zebrafish (*Danio rerio*)
737 larvae without live food: evaluation of a commercial, a practical
738 and a purified starter diet on larval performance. *Aquaculture*
739 *Research*, **37**(11), 1107-1111.

740 Castranova, D., Lawton, A., Lawrence, C., Baumann, D. P., Best, J.,
741 Coscolla, J., Doherty, A., Ramos, J., Hakkesteg, J., Wang, C.,
742 Wilson, J., Malley, J., & Wilson, C. (2011). The effect of stocking
743 densities on reproductive performance in laboratory zebrafish
744 (*Danio rerio*). *Zebrafish*, **8**(3), 141-146.

745 Cataudella, S., & Bronzi, P. (2001). *Acquacoltura Responsabile:*
746 *verso le produzioni acquatiche del terzo millennio*. Unimar -
747 Uniprom.

748 Clark, J. D., Gebhart, G. F., Gonder, J. C., Keeling, M. E., & Kohn, D.
749 F. (1997). The 1996 guide for the care and use of laboratory
750 animals. *ILAR journal*, **38**(1), 41-48.

751 Cooke, S. J., Chandroo, K. P., Beddow, T. A., Moccia, R. D., &
752 McKinley, R. S. (2000). Swimming activity and energetic
753 expenditure of captive rainbow trout *Oncorhynchus mykiss*
754 (Walbaum) estimated by electromyogram telemetry. *Aquaculture*
755 *Research*, **31**(6), 495-505.

756 Cabbage, C. C., & Mabee, P. M. (1996). Development of the cranium
757 and paired fins in the zebrafish *Danio rerio* (Ostariophysi,
758 Cyprinidae). *Journal of Morphology*, **229**(2), 121–160.

- 759 Danos, N., & Lauder, G. V. (2012). Challenging zebrafish escape
760 responses by increasing water viscosity. *Journal of Experimental*
761 *Biology*, **215**(11), 1854-1862.
- 762 De Clercq, A., Perrott, M. R., Davie, P. S., Preece, M. A., Wybourne,
763 B., Ruff, N., Huysseune, A., & Witten, P. E. (2017). Vertebral
764 column regionalisation in Chinook salmon, *Oncorhynchus*
765 *tshawytscha*. *Journal of anatomy*, **231**(4), 500-514.
- 766 Eastman, J. (1980). The caudal skeletons of catostomid fishes.
767 *American Midland Naturalist*, 133–148.
- 768 Eaton, R. C., & Emberley, D. S. (1991). How stimulus direction
769 determines the trajectory of the Mauthner-initiated escape
770 response in a teleost fish. *Journal of Experimental Biology*, **161**(1),
771 469-487.
- 772 Favaloro, E., & Mazzola, A. (2006). Meristic character counts and
773 incidence of skeletal anomalies in the wild *Diplodus puntazzo*
774 (Cetti, 1777) of an area of the south-eastern Mediterranean Sea.
775 *Fish Physiology and Biochemistry*, **32**(2), 159-166.
- 776 Ferreri, F., Nicolais, C., Boglione, C., & Bertolini, B. (2000). Skeletal
777 characterization of wild and reared zebrafish: anomalies and
778 meristic characters. *Journal of Fish Biology*, **56**(5), 1115-1128.
- 779 Fiaz, A. W., Léon-Kloosterziel, K. M., Gort, G., Schulte-Merker, S.,
780 van Leeuwen, J. L., & Kranenbarg, S. (2012). Swim-training
781 changes the spatio-temporal dynamics of skeletogenesis in
782 zebrafish larvae (*Danio rerio*). *PloS One*, **7**(4), e34072,
783 <https://doi.org/10.1371/journal.pone.0034072>.

- 784 Fiaz, A. W., van Leeuwen, J. L., & Kranenbarg, S. (2010).
785 Phenotypic plasticity and mechano-transduction in the teleost
786 skeleton. *Journal of Applied Ichthyology*, **26**(2), 289–293.
- 787 Fisher, S., Jagadeeswaran, P., & Halpern, M. E. (2003).
788 Radiographic analysis of zebrafish skeletal defects.
789 *Developmental Biology*, **264**(1), 64–76.
- 790 Fjelldal, P. G., Hansen, T., Breck, O., Ørnstrud, R., Lock, E.-J.,
791 Waagbø, R., Wargelius, A., & Witten, P. E. (2012). Vertebral
792 deformities in farmed Atlantic salmon (*Salmo salar* L.) - etiology
793 and pathology. *Journal of Applied Ichthyology*, **28**(3), 433–440.
- 794 Fjelldal, P. G., Hansen, T. J., & Berg, A. E. (2007). A radiological
795 study on the development of vertebral deformities in cultured
796 Atlantic salmon (*Salmo salar* L.). *Aquaculture*, **273**(4), 721–728.
- 797 Fleming, A., Keynes, R., & Tannahill, D. (2004). A central role for the
798 notochord in vertebral patterning. *Development*, **131**(4), 873-880.
- 799 Fleming, A., Kishida, M. G., Kimmel, C. B., & Keynes, R. J. (2015).
800 Building the backbone: the development and evolution of vertebral
801 patterning. *Development*, **142**(10), 1733-1744.
- 802 Gavaia, P. J., Dinis,
803 M. T., & Cancela, M. L. (2002). Osteological development and
804 abnormalities of the vertebral column and caudal skeleton in larval
805 and juvenile stages of hatchery-reared Senegal sole (*Solea
senegalensis*). *Aquaculture*, **211**(1-4), 305-323.
- 806 Gistelink, C., Witten, P. E., Huysseune, A., Symoens, S., Malfait, F.,
807 Larionova, D., Pascal Simoens, P., Dierick, M., Van Hoorebeke,
808 L., De Paepe, A., Kwon, R.Y., Weis, M., Eyre, D., R., Willaert, A.,
809 & Coucke, P.J. (2016). Loss of Type I Collagen Telopeptide Lysyl

810 Hydroxylation Causes Musculoskeletal Abnormalities in a
811 Zebrafish Model of Bruck Syndrome. *Journal of Bone and Mineral*
812 *Research*, **31**(11), 1930–1942.

813 Grini, A., Hansen, T., Berg, A., Wargelius, A., & Fjelldal, P. G. (2011).
814 The effect of water temperature on vertebral deformities and
815 vaccine-induced abdominal lesions in Atlantic salmon, *Salmo salar*
816 L. *Journal of fish diseases*, **34**(7), 531-546.

817 Goolish, E. M., Evans, R., Okutake, K., & Max, R. (1998). Chamber
818 volume requirements for reproduction of the zebrafish *Danio rerio*.
819 *The Progressive fish-culturist*, **60**(2), 127-132.

820 Gray, R. S., Wilm, T. P., Smith, J., Bagnat, M., Dale, R. M.,
821 Topczewski, J., Johnson, S.L., & Solnica-Krezel, L. (2014). Loss of
822 col8a1a function during zebrafish embryogenesis results in
823 congenital vertebral malformations. *Developmental Biology*,
824 **386**(1), 72–85.

825 Hall, B. K., & Witten, P. E. (2007). Plasticity of and transitions
826 between skeletal tissues in vertebrate evolution and development.
827 *Major transitions in vertebrate evolution*, 13-56.

828 Hall, B.K., & Witten, P.E. (2019). Plasticity and Variation of Skeletal
829 Cells and Tissues and the Evolutionary Development of
830 Actinopterygian Fishes. In: Z., Johanson, C., Underwood, M.,
831 Richter (Eds.) *Evolution and Development of Fishes* (pp. 126-143).
832 Cambridge University Press, Cambridge.

833 Haller, G., McCall, K., Jenkitkasemwong, S., Sadler, B., Antunes, L.,
834 Nikolov, M., Whittle, J., Upshaw, Z., Shin, J., Baschal, E.,
835 Cruchaga, C., Harms, M., Raggio, C., Morcuende, J.A.,

836 Giampietro, P., Miller, N.H., Wise, C., Gray, R.S., Solnica-Krezel,
837 L., Knutson, M., Dobbs, M.B., & Gurnett, C. A. (2018). A missense
838 variant in SLC39A8 is associated with severe idiopathic scoliosis.
839 *Nature Communications*, **9**(1), [https://doi.org/10.1038/s41467-018-](https://doi.org/10.1038/s41467-018-06705-0)
840 [06705-0](https://doi.org/10.1038/s41467-018-06705-0).

841 Hammer, Ø., Harper, D. A., & Ryan, P. D. (2001). PAST:
842 paleontological statistics software package for education and data
843 analysis. *Palaeontologia electronica*, **4**(1), 9.

844 Hayes, A. J., Reynolds, S., Nowell, M. A., Meakin, L. B., Habicher, J.,
845 Ledin, J., Bashford, A., Caterson, B., & Hammond, C. L. (2013).
846 Spinal deformity in aged zebrafish is accompanied by
847 degenerative changes to their vertebrae that resemble
848 osteoarthritis. *PLoS One*, **8**(9), 1–12.

849 Hazlerigg, C. R., Lorenzen, K., Thorbek, P., Wheeler, J. R., & Tyler,
850 C. R. (2012). Density-dependent processes in the life history of
851 fishes: evidence from laboratory populations of zebrafish *Danio*
852 *rerio*. *PLoS One*, **7**(5), e37550,
853 <https://doi.org/10.1371/journal.pone.0037550>.

854 Hennekam, R. C., Biesecker, L. G., Allanson, J. E., Hall, J. G., Opitz,
855 J. M., Temple, I. K., & Carey, J. C. (2013). Elements of
856 morphology: general terms for congenital anomalies. *American*
857 *Journal of Medical Genetics Part A*, **161**(11), 2726-2733.

858 Holm, J. C., Refstie, T., & Bø, S. (1990). The effect of fish density
859 and feeding regimes on individual growth rate and mortality in
860 rainbow trout (*Oncorhynchus mykiss*). *Aquaculture*, **89**(3-4), 225-
861 232.

- 862 Huysseune, A. (1995). Phenotypic plasticity in the lower pharyngeal
863 jaw dentition of *Astatoreochromis alluaudi* (Teleostei: Cichlidae).
864 *Archives of Oral Biology*, **40**(11), 1005-1014.
- 865 Huysseune, A., Sire, J. Y., & Meunier, F. J. (1994). Comparative
866 study of lower pharyngeal jaw structure in two phenotypes of
867 *Astatoreochromis alluaudi* (Teleostei: Cichlidae). *Journal of*
868 *Morphology*, **221**(1), 25-43.
- 869 Kihara, M., Ogata, S., Kawano, N., Kubota, I., & Yamaguchi, R.
870 (2002). Lordosis induction in juvenile red sea bream, *Pagrus*
871 *major*, by high swimming activity. *Aquaculture*, **212**(1-4), 149-158.
- 872 Klingenberg, C. P. (2019). Phenotypic plasticity, developmental
873 instability, and robustness: the concepts and how they are
874 connected. *Frontiers in Ecology and Evolution*, **7**, 56.
875 <https://doi.org/10.3389/fevo.2019.00056>
- 876 Koumoundouros, G., Gagliardi, F., Divanach, P., Boglione, C.,
877 Cataudella, S., & Kentouri, M. (1997). Normal and abnormal
878 osteological development of caudal fin in *Sparus aurata* L. fry.
879 *Aquaculture*, **149**(3-4), 215-226.
- 880 Kranenbarg, S., Waarsing, J., Muller, M., Weinans, H., & van
881 Leeuwen, J. (2005). Lordotic vertebrae in sea bass (*Dicentrarchus*
882 *labrax* L.) are adapted to increased loads. *Journal of*
883 *Biomechanics*, **38**(6), 1239–1246.
- 884 Laerm, J. (1979). On the origin of rhipidistian vertebrae. *Journal of*
885 *Paleontology*, 175-186.
- 886 Lawrence, C. (2007). The husbandry of zebrafish (*Danio rerio*): a
887 review. *Aquaculture*, **269**(1-4), 1-20.

- 888 Lawrence, C., & Mason, T. (2012). Zebrafish housing systems: a
889 review of basic operating principles and considerations for design
890 and functionality. *ILAR journal*, **53**(2), 179-191.
- 891 Liew, W. C., Bartfai, R., Lim, Z., Sreenivasan, R., Siegfried, K. R., &
892 Orban, L. (2012). Polygenic sex determination system in zebrafish.
893 *PLoS One*, **7**(4), e34397,
894 <https://doi.org/10.1371/journal.pone.0034397>.
- 895 Lisková, M., & Hert, J. (1971). Reaction of bone to mechanical
896 stimuli. 2. Periosteal and endosteal reaction of tibial diaphysis in
897 rabbit to intermittent loading. *Folia Morphologica*, **19**(3), 301–317.
- 898 Lleras Forero, L., Narayanan, R., Huitema, L. F. A., Vanbergen, M.,
899 Apschner, A., Peterson-Maduro, J., Logister, I., Valentin, G.,
900 Morelli, L.G., Oates, A.C., & Schulte-Merker, S. (2018).
901 Segmentation of the zebrafish axial skeleton relies on notochord
902 sheath cells and not on the segmentation clock. *eLife*, **7**, 1–28.
- 903 Matthews, M., Trevarrow, B., & Matthews, J. (2002). A virtual tour of
904 the guide for zebrafish users. *Resource*, **31**, 34-40.
- 905 Meyer, A. (1987). Phenotypic plasticity and heterochrony in
906 *Cichlasoma managuense* (Pisces, Cichlidae) and their implications
907 for speciation in cichlid fishes. *Evolution*, **41**(6), 1357-1369.
- 908 Nybelin, O. V. (1963). Zur morphologie und terminologie des
909 schwanzskelettes der Actinopterygier. *Arkiv för Zoologi*, **15**(35),
910 485-516.
- 911 Parichy, D. M., Elizondo, M. R., Mills, M. G., Gordon, T. N., &
912 Engeszer, R. E. (2009). Normal table of postembryonic zebrafish

913 development: Staging by externally visible anatomy of the living
914 fish. *Developmental Dynamics*, **238**(12), 2975–3015.

915 Pigliucci, M., Murren, C. J., & Schlichting, C. D. (2006). Phenotypic
916 plasticity and evolution by genetic assimilation. *The Journal of*
917 *experimental biology*, **209**(Pt 12).
918 <https://doi.org/10.1242/jeb.02070>.

919 Prestinicola, L., Boglione, C., Makridis, P., Spanò, A., Rimatori, V.,
920 Palamara, E., Scardi, M., & Cataudella, S. (2013). Environmental
921 Conditioning of Skeletal Anomalies Typology and Frequency in
922 Gilthead Seabream (*Sparus aurata* L., 1758) Juveniles. *PLoS*
923 *ONE*, **8**(2), e55736, <https://doi.org/10.1371/journal.pone.0055736>.

924 Ramsay, J. M., Feist, G. W., Varga, Z. M., Westerfield, M., Kent, M.
925 L., & Schreck, C. B. (2006). Whole-body cortisol is an indicator of
926 crowding stress in adult zebrafish, *Danio rerio*. *Aquaculture*,
927 **258**(1-4), 565-574.

928 Ribas, L., Valdivieso, A., Díaz, N., & Piferrer, F. (2017). Appropriate
929 rearing density in domesticated zebrafish to avoid masculinization:
930 links with the stress response. *Journal of Experimental Biology*,
931 **220**(6), 1056-1064.

932 Roo, J., Socorro, J., & Izquierdo, M. S. (2010). Effect of rearing
933 techniques on skeletal deformities and osteological development
934 in red porgy *Pagrus pagrus* (Linnaeus, 1758) larvae. *Journal of*
935 *Applied Ichthyology*, **26**(2), 372-376.

936 Roux W. (1881). Der züchtende Kampf der Teile, oder die
937 “Teilauslee” im Organismus (Theorie der “funktionellen
938 Anpassung”). Leipzig: Wilhelm Engelmann.

- 939 Rubin, C. T., & McLeod, K. J. (1994). Promotion of bony ingrowth by
940 frequency-specific, low-amplitude mechanical strain. *Clinical*
941 *Orthopaedics and Related Research*, **298**, 165–174.
- 942 Ruff, C., Holt, B., & Trinkaus, E. (2006). Who's afraid of the big bad
943 Wolff?: "Wolff's law" and bone functional adaptation. *American*
944 *Journal of Physical Anthropology: The Official Publication of the*
945 *American Association of Physical Anthropologists*, **129**(4), 484-
946 498.
- 947 Sæle, Ø., & Pittman, K. A. (2010). Looking closer at the determining
948 of a phenotype? Compare by stages or size, not age. *Journal of*
949 *Applied Ichthyology*, **26**(2), 294-297.
- 950 Schmalhausen, I. I. (1949). *Factors of evolution*. (Transl. by I Dordick.) Philadelphia.
- 951 Schindelin, J., Arganda-Carreras, I., Frise, E., Kaynig, V., Longair,
952 M., Pietzsch, T., Preibisch, S., Rueden, C., Saalfeld, S., Schmid,
953 B., Tinevez, J-Y., White, D. J., Hartenstein, V., Eliceiri, K.,
954 Tomancak, P., & Cardona, A. (2012), "Fiji: an open-source
955 platform for biological-image analysis", *Nature methods*, **9**(7): 676-
956 682
- 957 Schmalhausen, I. I. (1949). *Factors of evolution*. (Transl. by I
958 Dordick.) Philadelphia.
- 959 Sfakianakis, D. G., Leris, I., Laggis, A., & Kentouri, M. (2011). The
960 effect of rearing temperature on body shape and meristic
961 characters in zebrafish (*Danio rerio*) juveniles. *Environmental*
962 *Biology of Fishes*, **92**(2), 197–205.
- 963 Shadwick, R. E., & Lauder, G. V. (Eds.). (2006). *Fish physiology:*
964 *Fish biomechanics* (Vol. 23). Elsevier.

- 965 Shelton, D. S., Price, B. C., Ocasio, K. M., & Martins, E. P. (2015).
966 Density and group size influence shoal cohesion, but not
967 coordination in zebrafish (*Danio rerio*). *Journal of Comparative*
968 *Psychology*, **129**(1), 72-77.
- 969 Slijper, E. J. (1942). Biologic anatomical investigations on the bipedal
970 gait and upright posture in mammals-With special reference to a
971 little goat born without forelegs II. *Proceedings of the Koninklijke*
972 *Nederlandse Akademie Van Wetenschappen*, **45**(1/5), 407-415.
- 973 Spoorendonk, K. M., Peterson-Maduro, J., Renn, J., Trowe, T.,
974 Kranenbarg, S., Winkler, C., & Schulte-Merker, S. (2008). Retinoic
975 acid and Cyp26b1 are critical regulators of osteogenesis in the
976 axial skeleton. *Development*, **135**(22), 3765-3774. Suniaga, S.,
977 Rolvien, T., Vom Scheidt, A., Fiedler, I. A. K., Bale, H. A.,
978 Huysseune, A., Witten, P.E., Amling, M., & Busse, B. (2018).
979 Increased mechanical loading through controlled swimming
980 exercise induces bone formation and mineralization in adult
981 zebrafish. *Scientific Reports*, **8**(1), 1–13.
- 982 Taylor, W. R., & Van Dyke, G. C. (1985). Revised procedures for
983 staining and clearing small fishes and other vertebrates for bone
984 and cartilage study. *Cybium*, **9**, 107-119
- 985 Tibile, R. M., Sawant, P. B., Chadha, N. K., Lakra, W. S., Prakash,
986 C., Swain, S., & Bhagawati, K. (2016). Effect of stocking density
987 on growth, size variation, condition index and survival of discus,
988 *Symphysodon aequifasciatus* Pellegrin, 1904. *Turkish Journal of*
989 *Fisheries and Aquatic Sciences*, **16**(2), 453-460.

990 Tsang, B., Zahid, H., Ansari, R., Lee, R. C. Y., Partap, A., & Gerlai,
991 R. (2017). Breeding zebrafish: a review of different methods and a
992 discussion on standardization. *Zebrafish*, **14**(6), 561-573.

993 Turner, C H, Forwood, M. R., & Otter, M. W. (1994a).
994 Mechanotransduction in bone: do bone cells act as sensors of fluid
995 flow? *The FASEB Journal*, **8**(11), 875–878.

996 Turner, C. H. (1998). Three rules for bone adaptation to mechanical
997 stimuli. *Bone*, **23**(5), 399–407.

998 Turner, C. H., Owan, I., & Takano, Y. (1995). Mechanotransduction
999 in bone: role of strain rate. *American Journal of Physiology-
1000 Endocrinology and Metabolism*, **269**(3), E438–E442.

1001 Turner, Charles H., Forwood, M. R., Rho, J.-Y., & Yoshikawa, T.
1002 (1994b). Mechanical loading thresholds for lamellar and woven
1003 bone formation. *Journal of Bone and Mineral Research*, **9**(1), 87–
1004 97.

1005 van der Meulen, T. (2005). *Epigenetics of the locomotory system in
1006 zebrafish*. (Doctoral thesis, Wageningen University, The
1007 Netherlands). Retrieved from
1008 <https://library.wur.nl/WebQuery/wurpubs/fulltext/121740>

1009 van Eeden, F. J. M., Granato, M., Schach, U., Brand, M., Furutani-
1010 Seiki, M., Haffter, P., Hammerschmidt, M., Heisenberg, C. P.,
1011 Jiang, Y. J., Kane, D. A., Kelsh, R. N., Mullins, M. C., Odenthal,
1012 J., Warga, R. M., Nüsslein-Volhard, C. (1996). Genetic analysis of
1013 fin formation in the zebrafish, *Danio rerio*. *Development* **123**, 255-
1014 262.

- 1015 Waddington, C. H. (1953). Genetic assimilation of an acquired
1016 character. *Evolution*, **7**(2), 118-126.
- 1017 Wakeling, J. M., & Johnston, I. A. (1999). Body bending during fast-
1018 starts in fish can be explained in terms of muscle torque and
1019 hydrodynamic resistance. *The Journal of Experimental Biology*,
1020 **202**(1), 675–682.
- 1021 Wargelius, A., Fjellidal, P. G., & Hansen, T. (2005). Heat shock during
1022 early somitogenesis induces caudal vertebral column defects in
1023 Atlantic salmon (*Salmo salar*). *Development genes and
1024 evolution*, **215**(7), 350-357.
- 1025 Weinans, H., & Prendergast, P. J. (1996). Tissue adaptation as a
1026 dynamical process far from equilibrium. *Bone*, **19**(2), 143-149.
- 1027 West-Eberhard, M. J. (2003). *Developmental plasticity and evolution*.
1028 Oxford University Press.
- 1029 West-Eberhard, M. J. (2005). Phenotypic accommodation: adaptive
1030 innovation due to developmental plasticity. *Journal of
1031 Experimental Zoology Part B: Molecular and Developmental
1032 Evolution*, **304**(6), 610-618.
- 1033 Westerfield, M. (2000). *The zebrafish book: a guide for the laboratory
1034 use of zebrafish*. 4th Edition, University of Oregon Press, Eugene
- 1035 Witten, P. E., & Hall, B. K. (2015). Teleost skeletal plasticity:
1036 modulation, adaptation, and remodelling. *Copeia*, **103**(4), 727-739.
- 1037 Witten, P. E., Gil-Martens, L., Hall, B. K., Huysseune, A., & Obach, A.
1038 (2005). Compressed vertebrae in Atlantic salmon *Salmo salar*.
1039 evidence for metaplastic chondrogenesis as a skeletogenic

1040 response late in ontogeny. *Diseases of aquatic organisms*, **64**(3),
1041 237-246.

1042 Witten, P. E., Obach, A., Huysseune, A., & Baeverfjord, G. (2006).
1043 Vertebrae fusion in Atlantic salmon (*Salmo salar*): Development,
1044 aggravation and pathways of containment. *Aquaculture*, **258**(1–4),
1045 164–172.

1046 Witten, P. E., Harris, M. P., Huysseune, A., & Winkler, C. (2017).
1047 Small teleost fish provide new insights into human skeletal
1048 diseases. In *Methods in cell biology* (Vol. 138, pp. 321-346).
1049 Academic Press.

1050 Witten, P. E., Huysseune, A., & Hall, B. K. (2010). A practical
1051 approach for the identification of the many cartilaginous tissues in
1052 teleost fish. *Journal of Applied Ichthyology*, **26**(2), 257-262.

1053 Witten, P. E., Obach, A., Huysseune, A., & Baeverfjord, G. (2006).
1054 Vertebrae fusion in Atlantic salmon (*Salmo salar*): development,
1055 aggravation and pathways of containment. *Aquaculture*, **258**(1-4),
1056 164-172.

1057 Wolff, J. (1892). *The law of bone transformation*. Berlin: Hirschwald.

1058 Wopat, S., Bagwell, J., Sumigray, K. D., Dickson, A. L., Huitema, L.
1059 F. A., Poss, K. D., Schulte-Merker, S., & Bagnat, M. (2018). Spine
1060 Patterning Is Guided by Segmentation of the Notochord Sheath.
1061 *Cell Reports*, **22**(8), 2094–2106.

1062 Ytteborg, E., Torgersen, J., Baeverfjord, G., & Takle, H. (2010).
1063 Morphological and molecular characterization of developing
1064 vertebral fusions using a teleost model. *BMC physiology*, **10**(1),
1065 13, <https://doi.org/10.1186/1472-6793-10-13>.

1066 Zouiten, D., Ben Khemis, I., Slaheddin Masmoudi, A., Huelvan, C., &
1067 Cahu, C. (2011). Comparison of growth, digestive system
1068 maturation and skeletal development in sea bass larvae reared in
1069 an intensive or a mesocosm system. *Aquaculture Research*,
1070 **42**(11), 1723–1736.

Region	Skeletal element	code	Description
A			Weberian vertebrae (carrying modified arches/spines- Weberian ossicles)
B			Abdominal vertebrae (carrying ribs and open haemal arches, without haemal spines)
C			Caudal vertebrae (with closed haemal and neural arches/spines)
D			Caudal complex (preurals and ural vertebrae)
E			Pectoral fin
F			Anal fin
G			Caudal fin
H			Dorsal fin
I			Pelvic fin
	1	kyp lor sbs sco	Kyphosis Lordosis Saddle-back syndrome* Scoliosis
	2	par fus def elo/red	Partial vertebral fusion Complete vertebral body-centra fusion Vertebral deformation Vertebral marked elongation/reduction in length
	3	def dec	Deformed urostyle Unmineralized urostyle
	4	def sup/abs sup/abs (L/R) bif mis ins	Malformed neural arch and/or spine Supernumerary/absent neural elements Supernumerary/absent left/right neural elements Bifid (forked) neural spine, the right and the left spine don't fuse Mismatched fusion of two different neural spines Misplacement of the neural arch insertion
	5	def sup/abs sup/abs (L/R) bif mis ins	Malformed haemal arch and/or spine Supernumerary/absent haemal elements Supernumerary/absent left/right haemal elements Bifid (forked) haemal spine, the right and the left spine don't fuse Mismatched fusion of two different haemal spines Misplacement of the haemal arch insertion
	6	def	Deformed Weberian ossicles
	7	def sup/abs	Malformed rib Supernumerary/ absent pleural rib
	8	def sup/abs fus dec	Deformed fin ray inner support Supernumerary/absent fin ray inner support Fused fin ray inner support Unmineralized fin ray inner support
	9	def sup/abs fus dec	Deformed hypural Supernumerary/absent hypural Fused hypural Unmineralized hypural
	10	def dec fus	Deformed parahypural Unmineralized parahypural Fused parahypural
	11	def sup/abs fus dec	Deformed epural Supernumerary/absent epural Fused epural Unmineralized epural
	12	def sup/abs fus	Deformed ray Supernumerary/absent ray Fused ray
	13	def	Malformed maxillary and/or pre-maxillary
	14	def	Malformed dentary
	15	def	Other cephalic deformities (glossohyal, neurocranium...)
	16	def L/R	Malformed left/right operculum
	17	def L/R sup/abs (L/R) fus L/R	Deformed branchiostegal ray - L/R Supernumerary/absent branchiostegal ray - L/R Fused branchiostegal ray - L/R
	18	def	Supraneurals bones malformations

	sup/abs	Supernumerary/absent supraneurals
	fus	Fused supraneurals
	dec	Unmineralized supraneurals
19	def	Malformed cleithrum L/R
20	def	Malformed left/right coracoids
21	def	Deformed postcleithrum

Codes for grouped anomalies

Ac	Centra of the Weberian region
Aae	Centra-associated elements (arches and Weberian ossicles) of the Weberian region
Bc	Centra of the abdominal region
Bae	Centra-associated elements (arches and spines) of the abdominal region
Cc	Centra of the caudal region
Cae	Centra-associated elements (arches and spines) of the caudal region
Dc	Centra of the caudal complex
Dae	Centra-associated elements (arches and spines) of the caudal complex

Table 1 List of the anomalies considered. In red, severe anomalies. Skeletal elements codes: 1 = vertebral column; 2 = vertebral centrum; 3 = urostyle; 4 = neural arch and spine; 5 = haemal arch and spine; 6 = Weberian ossicles; 7 = rib; 8 = internal support of fin rays; 9 = hypural; 10 = parahypural; 11 = epural; 12 = ray; 13 = maxillary and/or pre-maxillary; 14 = dentary; 15 = other cephalic anomalies; 16 = operculum; 17 = branchiostegal ray; 18 = supraneural bone; 19 = cleithrum; 20 = coracoid; 21 = postcleithrum.

**Saddle-back syndrome refers to the deformation of the dorsal profile (shaped as a "saddle") linked to the lack of dorsal fin pterygiophores and rays. It can be associated to deformed caudal fin, abdominal kyphosis, caudal lordosis and caudal fin anomalies.*

		Pectoral fin					Pelvic fin		Dorsal fin		Anal fin		Caudal fin				
		Vertebral [red box]	Supraneurals	Left radials	Right radials	Left rays	Right rays	Left rays	Right rays	Pterygiophores	Rays	Pterygiophores	Rays	Epural	Hypurals and parahypural	Upper rays	Lower rays
T0	Modal value	34	7	4	4	10	10	6	5	8	8	13	14	1	6	9	9
	Range	32-35	0-8			5-10	5-11	5-8	4-8	5-8	5-10	7-14	7-16			8-9	8-9
	Specimens with incomplete development of skeletal elements	2/32	26/32	15/32		32/32		30/32		5/32	20/32	15/32	25/32	0/32	0/32		0/32
HD	Modal value	33	7	4	4	12	12	8	8	8	9	13	15	1	6	9	9
	Range	30-36	4-11	3-4		10-13	10-13	6-8	6-9	7-8	9-10	12-15	13-17			8-10	8-10
MD	Modal value	34	7	4	4	12	12	8	8	8	9	13	15	1	6	9	9
	Range	33-36	4-10		3-4	10-14	11-14	6-8	6-8	7-8	9-10	10-15	11-17	0-1	5-6	7-9	8-10
LD	Modal value	34	7	4	4	12	12	8	8	8	9	13	15	1	6	9	9
	Range	32-35	6-9			12-13	12-13	7-8	7-8	7-9	8-9	12-15	14-17		5-6	7-9	7-9

Table 2 Modal values and range for the vertebral [red box] and fins' elements in the T0 and the three experimental groups. Ranges left empty indicate no variation in the number of elements. Note that lower modal values reported for some skeletal element in the T0 group compared to the experimental groups are due to the incomplete development of such skeletal elements at the considered stage (T0, 30 dpf). [The third row for the T0 samples](#) "Specimens with incomplete development of skeletal elements" indicates the number of individuals on the total of T0 group (n = 32) having not yet differentiated the final numbers of skeletal elements.

<i>General metrics on skeletal anomalies</i>	T0
N of observed specimens	32
Frequency (%) of specimens with at least one anomaly	56
Average anomaly load	9
N of observed types of anomaly	17
Frequency (%) of specimens with at least one severe anomaly	34
Average severe anomaly load	2
Frequency (%) of observed severe anomalies/total n anomalies	12

Table 3 General metrics for the analysis of the skeletal anomalies for the T0 group.

<i>General metrics on skeletal anomalies</i>	HD	MD	LD
N observed specimens	65	46	19
Frequency (%) of specimens with at least one anomaly	100	98	100
Average anomaly load	12	9	9
N observed types of anomaly	68	47	44
Frequency (%) of specimens with at least one severe anomaly	72	73	58
Average severe anomaly load	2	3	3
Frequency (%) of severe anomalies/total n anomalies	13	21	19

Table 4 General metrics for the analysis of skeletal anomalies in the experimental groups HD, MD and LD. Highest values are shown in bold.

Region	Skeletal element	code	Description
A			Weberian vertebrae (carrying modified arches/spines- Weberian ossicles)
B			Abdominal vertebrae (carrying ribs and open haemal arches, without haemal spines)
C			Caudal vertebrae (with closed haemal and neural arches/spines)
D			Caudal complex (preurals and ural vertebrae)
E			Pectoral fin
F			Anal fin
G			Caudal fin
H			Dorsal fin
I			Pelvic fin
	1	kyp lor sbs sco	Kyphosis Lordosis Saddle-back syndrome* Scoliosis
	2	par fus def elo/red	Partial vertebral fusion Complete vertebral centra fusion Vertebral deformation Vertebral marked elongation/reduction in length
	3	def dec	Deformed urostyle Unmineralized urostyle
	4	def sup/abs sup/abs (L/R) bif mis ins	Malformed neural arch and/or spine Supernumerary/absent neural elements Supernumerary/absent left/right neural elements Bifid (forked) neural spine, the right and the left spine don't fuse Mismatched fusion of two different neural spines Misplacement of the neural arch insertion
	5	def sup/abs sup/abs (L/R) bif mis ins	Malformed haemal arch and/or spine Supernumerary/absent haemal elements Supernumerary/absent left/right haemal elements Bifid (forked) haemal spine, the right and the left spine don't fuse Mismatched fusion of two different haemal spines Misplacement of the haemal arch insertion
	6	def	Deformed Weberian ossicles
	7	def sup/abs	Malformed rib Supernumerary/ absent pleural rib
	8	def sup/abs fus dec	Deformed fin ray inner support Supernumerary/absent fin ray inner support Fused fin ray inner support Unmineralized fin ray inner support
	9	def sup/abs fus dec	Deformed hypural Supernumerary/absent hypural Fused hypural Unmineralized hypural
	10	def dec fus	Deformed parahypural Unmineralized parahypural Fused parahypural
	11	def sup/abs fus dec	Deformed epural Supernumerary/absent epural Fused epural Unmineralized epural
	12	def sup/abs fus	Deformed ray Supernumerary/absent ray Fused ray
	13	def	Malformed maxillary and/or pre-maxillary
	14	def	Malformed dentary
	15	def	Other cephalic deformities (glossohyal, neurocranium...)
	16	def L/R	Malformed left/right operculum
	17	def L/R sup/abs (L/R) fus L/R	Deformed branchiostegal ray - L/R Supernumerary/absent branchiostegal ray - L/R Fused branchiostegal ray - L/R
	18	def	Supraneurals bones malformations

	sup/abs	Supernumerary/absent supraneurals
	fus	Fused supraneurals
	dec	Unmineralized supraneurals
19	def	Malformed cleithrum L/R
20	def	Malformed left/right coracoids
21	def	Deformed postcleithrum

Codes for grouped anomalies

Ac	Centra of the Weberian region
Aae	Centra-associated elements (arches and Weberian ossicles) of the Weberian region
Bc	Centra of the abdominal region
Bae	Centra-associated elements (arches and spines) of the abdominal region
Cc	Centra of the caudal region
Cae	Centra-associated elements (arches and spines) of the caudal region
Dc	Centra of the caudal complex
Dae	Centra-associated elements (arches and spines) of the caudal complex

Table 1 List of the anomalies considered. In red, severe anomalies. Skeletal elements codes: 1 = vertebral column; 2 = vertebral centrum; 3 = urostyle; 4 = neural arch and spine; 5 = haemal arch and spine; 6 = Weberian ossicles; 7 = rib; 8 = internal support of fin rays; 9 = hypural; 10 = parahypural; 11 = epural; 12 = ray; 13 = maxillary and/or pre-maxillary; 14 = dentary; 15 = other cephalic anomalies; 16 = operculum; 17 = branchiostegal ray; 18 = supraneural bone; 19 = cleithrum; 20 = coracoid; 21 = postcleithrum.

**Saddle-back syndrome refers to the deformation of the dorsal profile (shaped as a "saddle") linked to the lack of dorsal fin pterygiophores and rays. It can be associated to deformed caudal fin, abdominal kyphosis, caudal lordosis and caudal fin anomalies.*

		<i>Pectoral fin</i>					<i>Pelvic fin</i>		<i>Dorsal fin</i>		<i>Anal fin</i>		<i>Caudal fin</i>				
		<i>Vertebral centra</i>	<i>Supraneurals</i>	<i>Left radials</i>	<i>Right radials</i>	<i>Left rays</i>	<i>Right rays</i>	<i>Left rays</i>	<i>Right rays</i>	<i>Pterygiophores</i>	<i>Rays</i>	<i>Pterygiophores</i>	<i>Rays</i>	<i>Epural</i>	<i>Hypurals and parahypural</i>	<i>Upper rays</i>	<i>Lower rays</i>
T0	<i>Modal value</i>	34	7	4	4	10	10	6	5	8	8	13	14	1	6	9	9
	<i>Range</i>	32-35	0-8			5-10	5-11	5-8	4-8	5-8	5-10	7-14	7-16			8-9	8-9
	<i>Specimens with incomplete development of skeletal elements</i>	2/32	26/32	15/32		32/32		30/32		5/32	20/32	15/32	25/32	0/32	0/32		0/32
HD	<i>Modal value</i>	33	7	4	4	12	12	8	8	8	9	13	15	1	6	9	9
	<i>Range</i>	30-36	4-11	3-4		10-13	10-13	6-8	6-9	7-8	9-10	12-15	13-17			8-10	8-10
MD	<i>Modal value</i>	34	7	4	4	12	12	8	8	8	9	13	15	1	6	9	9
	<i>Range</i>	33-36	4-10		3-4	10-14	11-14	6-8	6-8	7-8	9-10	10-15	11-17	0-1	5-6	7-9	8-10
LD	<i>Modal value</i>	34	7	4	4	12	12	8	8	8	9	13	15	1	6	9	9
	<i>Range</i>	32-35	6-9			12-13	12-13	7-8	7-8	7-9	8-9	12-15	14-17		5-6	7-9	7-9

Table 2 Modal values and range for the vertebral centra and fins' elements in the T0 and the three experimental groups. Ranges left empty indicate no variation in the number of elements. Note that lower modal values reported for some skeletal element in the T0 group compared to the experimental groups are due to the incomplete development of such skeletal elements at the considered stage (T0, 30 dpf). "Specimens with incomplete development of skeletal elements" indicates the number of individuals on the total of T0 group (n = 32) having not yet differentiated the final numbers of skeletal elements.

<i>General metrics on skeletal anomalies</i>	T0
N of observed specimens	32
Frequency (%) of specimens with at least one anomaly	56
Average anomaly load	9
N of observed types of anomaly	17
Frequency (%) of specimens with at least one severe anomaly	34
Average severe anomaly load	2
Frequency (%) of observed severe anomalies/total n anomalies	12

Table 3 General metrics for the analysis of the skeletal anomalies for the T0 group.

<i>General metrics on skeletal anomalies</i>	HD	MD	LD
N observed specimens	65	46	19
Frequency (%) of specimens with at least one anomaly	100	98	100
Average anomaly load	12	9	9
N observed types of anomaly	68	47	44
Frequency (%) of specimens with at least one severe anomaly	72	73	58
Average severe anomaly load	2	3	3
Frequency (%) of severe anomalies/total n anomalies	13	21	19

Table 4 General metrics for the analysis of skeletal anomalies in the experimental groups HD, MD and LD. Highest values are shown in bold.

Figure 1 Histogram showing the frequency of each malformation on the total of the observed malformations and the frequency of affected specimens in the T0 group.

Figure 2 Box plot for the S_L in HD, MD and LD experimental groups. The box represents the 25-75 percent quartiles, the horizontal line inside the box indicates the median value, the cross indicates the mean value and the minimal and maximal values are shown with “whiskers”. A dot indicates outlier, defined as data value larger or smaller than 1.5 times the interquartile range. All the differences between groups, are significant according to Kruskal-Wallis test, followed by Dunn’s post hoc test with Bonferroni correction ($p < 0.01$), as indicated by different letters.

Figure 3 Histograms showing the frequency of deformities grouped per typology of skeletal element and region (a) and the frequency of specimens affected (b), for each experimental group. Aae: deformities of the centra-associated elements in the Weberian region; Ac: deformities of the centra in the Weberian region; Bae: deformities of the centra-associated elements in the abdominal region; Bc: deformities of the centra in the abdominal region; Cae: deformities of the centra-associated elements in the caudal region; Cc: deformities of the centra in the caudal region; Dae: deformities of the centra-associated elements in the caudal complex; Dc: deformities of the centra in the caudal complex.

Figure 4 Histograms showing the frequency of deformities (a) and affected specimens (b) in the caudal region.

Figure 5 Some of the recorded deformities: a) normal vertebrae; b) B4def, neural arches and spines deformities in the abdominal region and B7def, anomalous ribs; c) C4abs L, missing left neural arch in the caudal region, C4bif, bifid neural spine in the caudal region, C5def, anomalous haemal arches and spines in the caudal region; d) C2fus, complete vertebral body fusion in the caudal region; e) C2par, partial vertebral body’s fusion; f) C4ins, misplacement of the neural arch insertion in a caudal vertebra, F8def, deformed anal fin’s pterygiophores, C5abs, absence of the haemal arch in a caudal vertebra; g) D2fus, complete fusion in the caudal complex; h) G11def, deformation of the epural. Alizarin red whole-mount staining.

Figure 6 Ordination model obtained by CA applied to a subset of RM (matrix 57x12). Dots represent individuals, each one of them is connected with a line to the centroid (i.e., the average of x and y-axes coordinates of individuals belonging to each experimental group). Experimental groups and deformities are plotted in separate graphs (a-d) to allow better the visualization.

Figure 1 Histogram showing the frequency of each malformation on the total of the observed malformations and the frequency of affected specimens in the T0 group.

Figure 2 Box plot for the S_L in HD, MD and LD experimental groups. The box represents the 25-75 percent quartiles, the horizontal line inside the box indicates the median value, the cross indicates the mean value and the minimal and maximal values are shown with “whiskers”. A dot indicates outlier, defined as data value larger or smaller than 1.5 times the interquartile range. All the differences between groups, are significant according to Kruskal-Wallis test, followed by Dunn’s post hoc test with Bonferroni correction ($p < 0.01$), as indicated by different letters.

Figure 3 Histograms showing the frequency of deformities grouped per typology of skeletal element and region (a) and the frequency of specimens affected (b), for each experimental group. Aae: deformities of the centra-associated elements in the Weberian region; Ac: deformities of the centra in the Weberian region; Bae: deformities of the centra-associated elements in the abdominal region; Bc: deformities of the centra in the abdominal region; Cae: deformities of the centra-associated elements in the caudal region; Cc: deformities of the centra in the caudal region; Dae: deformities of the centra-associated elements in the caudal complex; Dc: deformities of the centra in the caudal complex.

Figure 4 Histograms showing the frequency of deformities (a) and affected specimens (b) in the caudal region.

Figure 5 Some of the recorded deformities: a) normal vertebrae; b) B4def, neural arches and spines deformities in the abdominal region and B7def, anomalous ribs; c) C4abs L, missing left neural arch in the caudal region, C4bif, bifid neural spine in the caudal region, C5def, anomalous haemal arches and spines in the caudal region; d) C2fus, complete vertebral body fusion in the caudal region; e) C2par, partial vertebral body’s fusion; f) C4ins, misplacement of the neural arch insertion in a caudal vertebra, F8def, deformed anal fin’s pterygiophores, C5abs, absence of the haemal arch in a caudal vertebra; g) D2fus, complete fusion in the caudal complex; h) G11def, deformation of the epural. Alizarin red whole-mount staining.

Figure 6 Ordination model obtained by CA applied to a subset of RM (matrix 57x12). Dots represent individuals, each one of them is connected with a line to the centroid (i.e., the average of x and y-axes coordinates of individuals belonging to each experimental group). Experimental groups and deformities are plotted in separate graphs (a-d) to allow better the visualization.

Figure 1

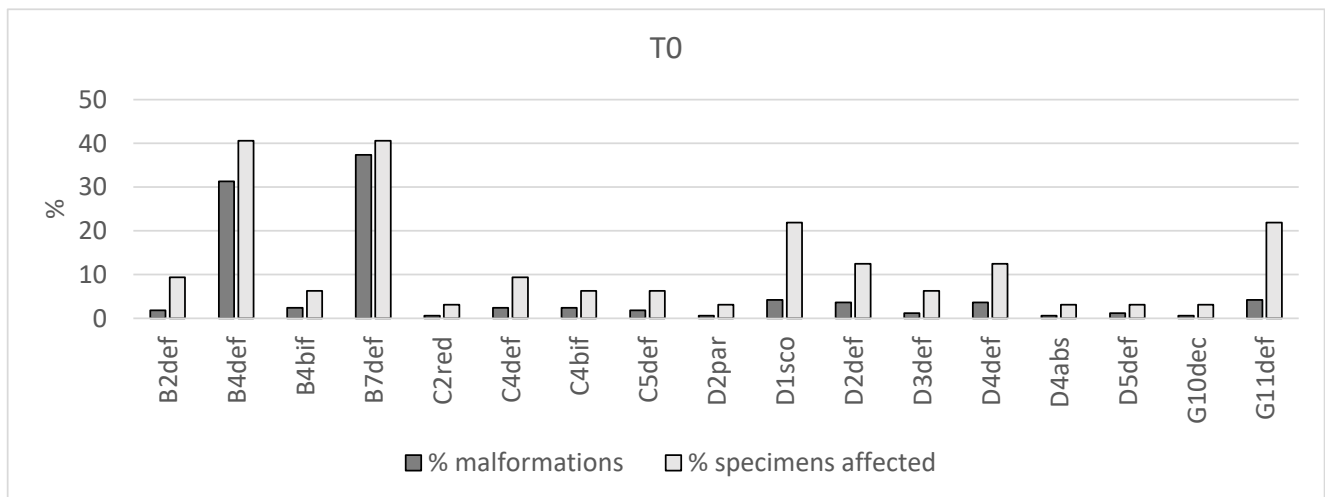


Figure 2

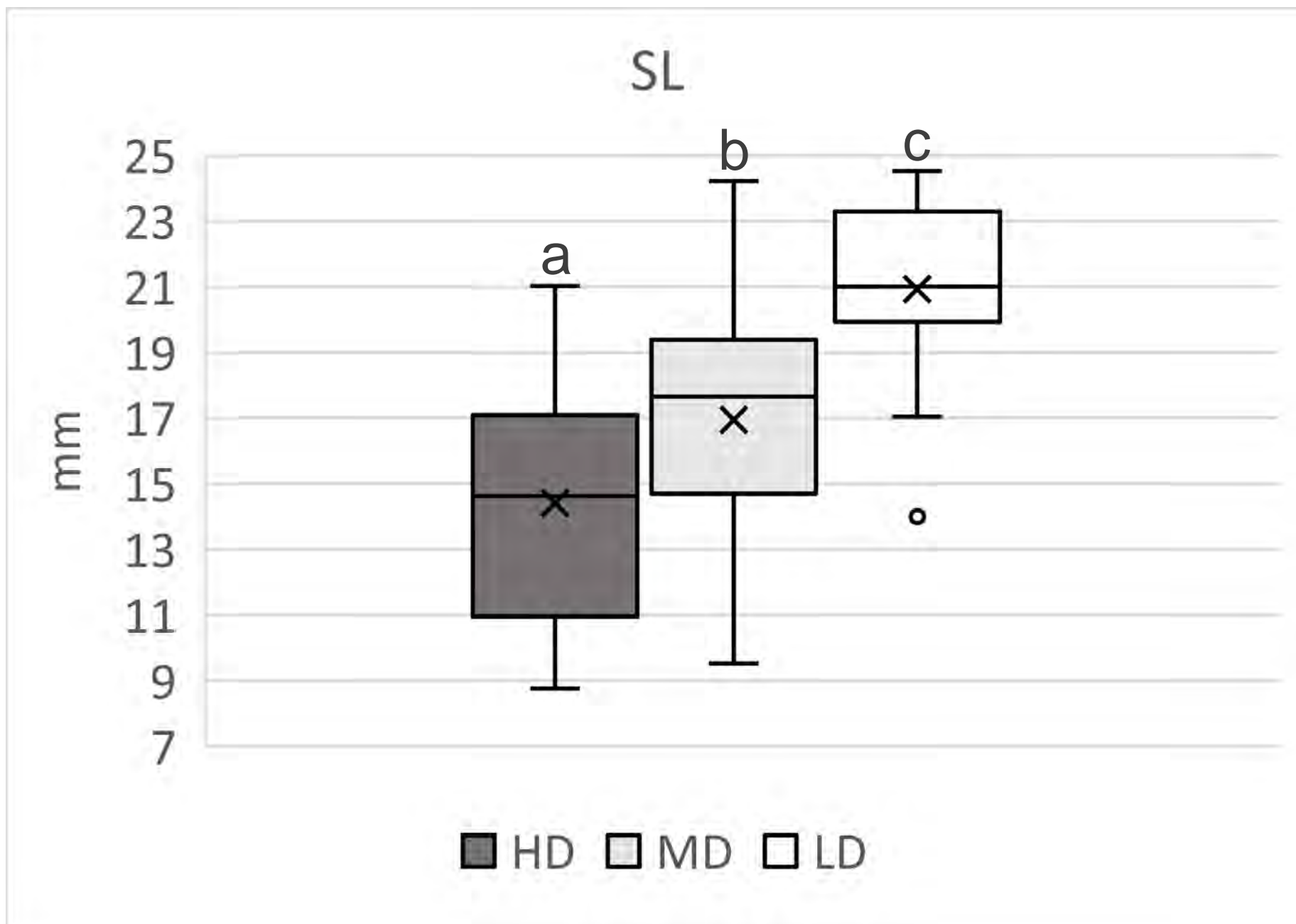


Figure 3

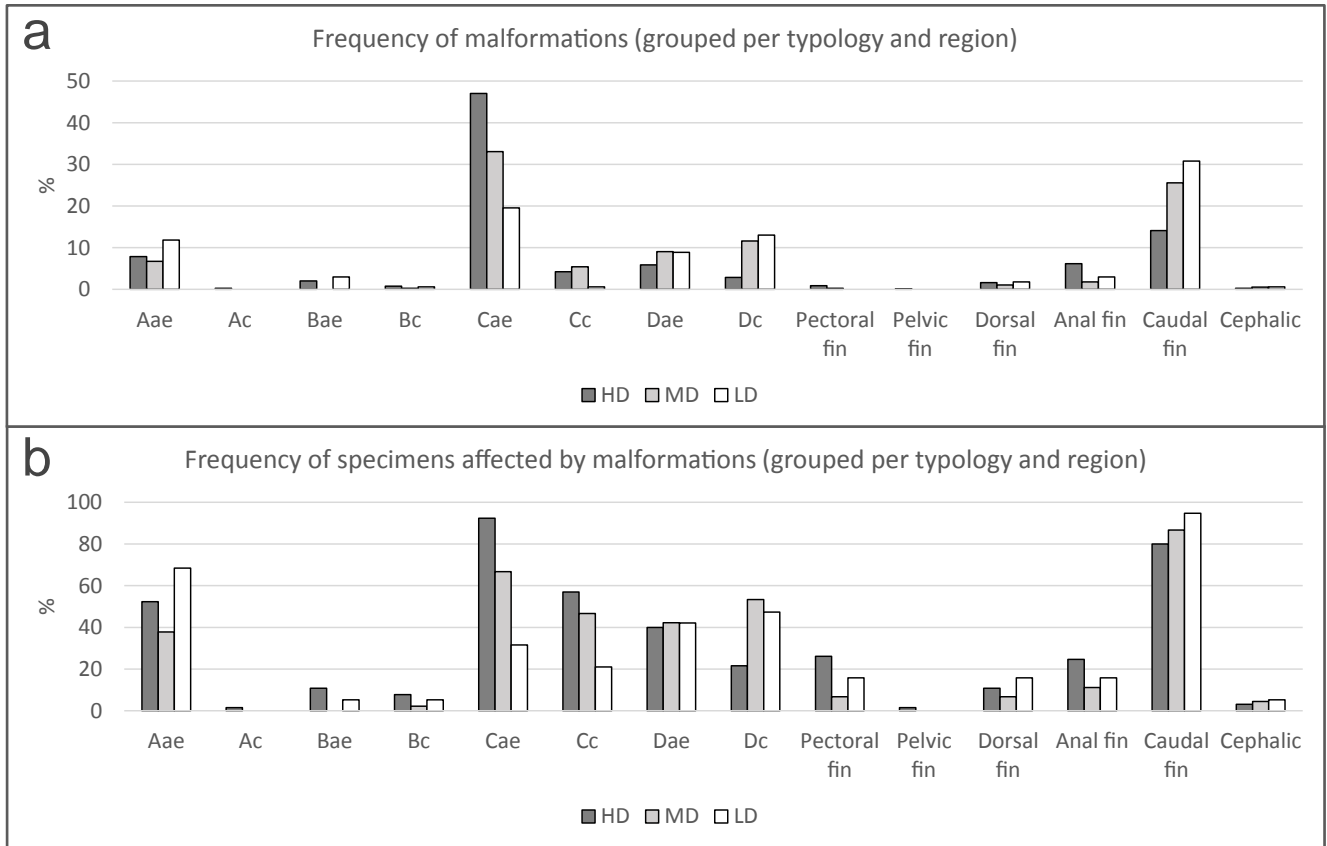
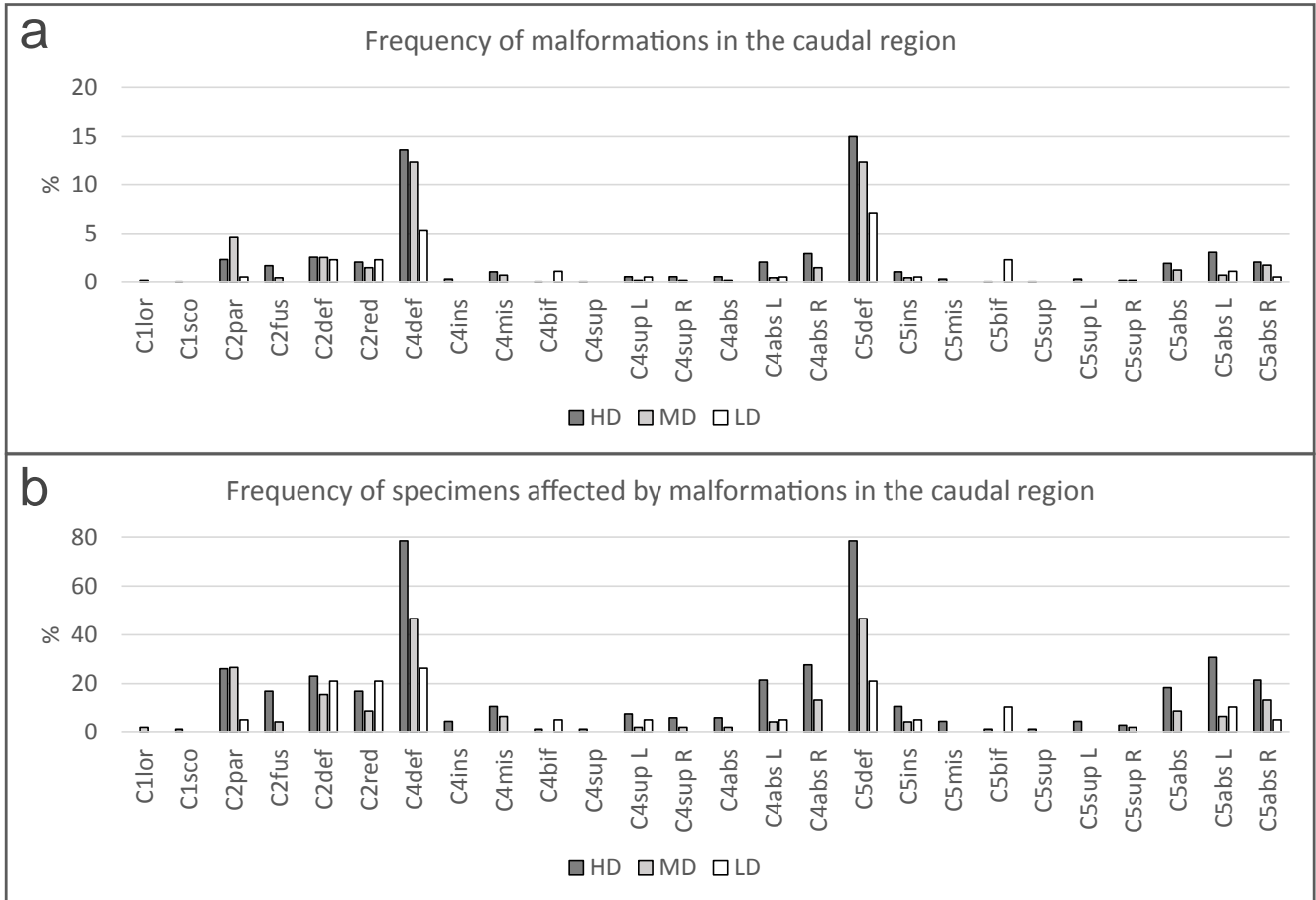


Figure 4



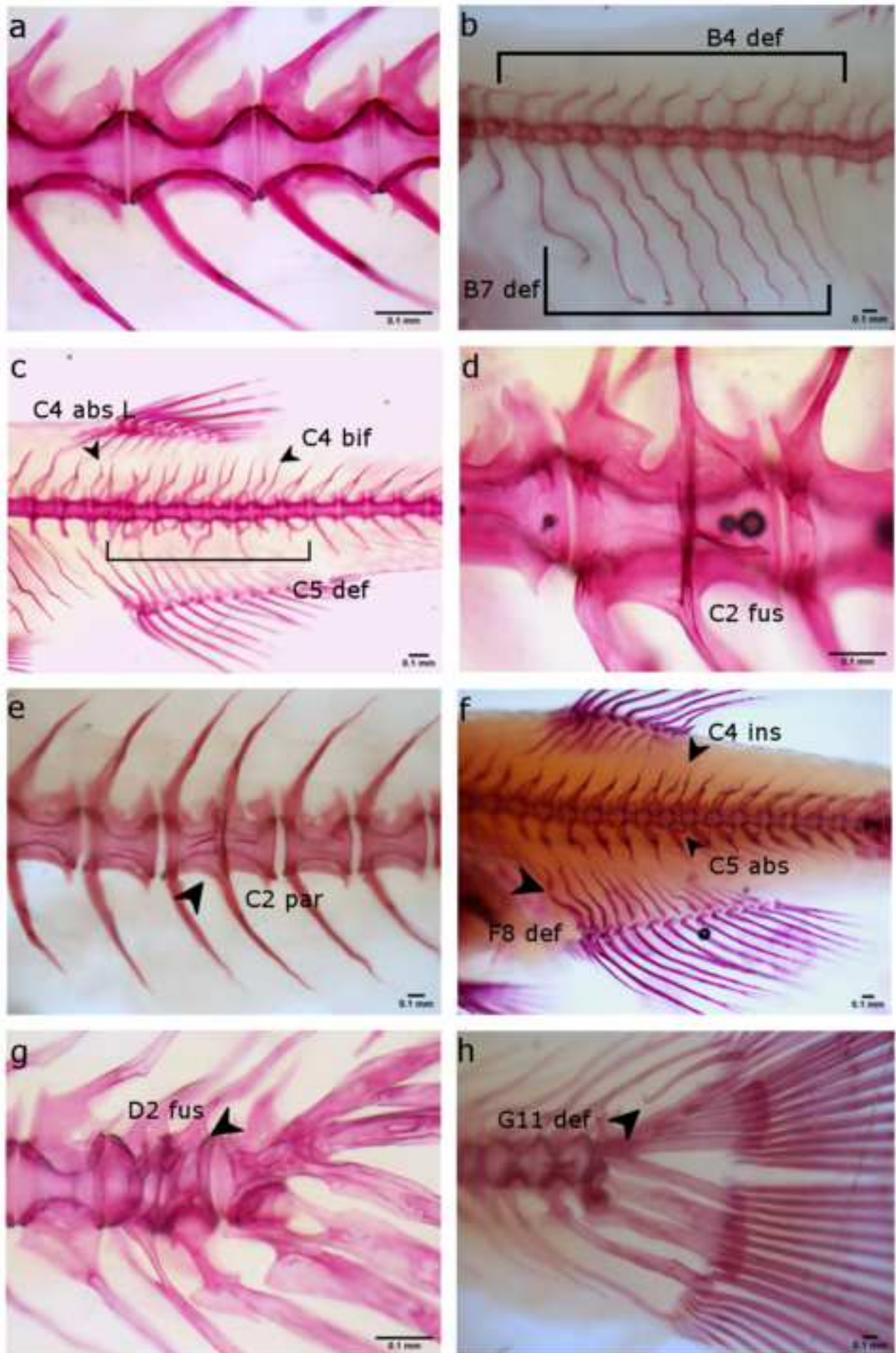
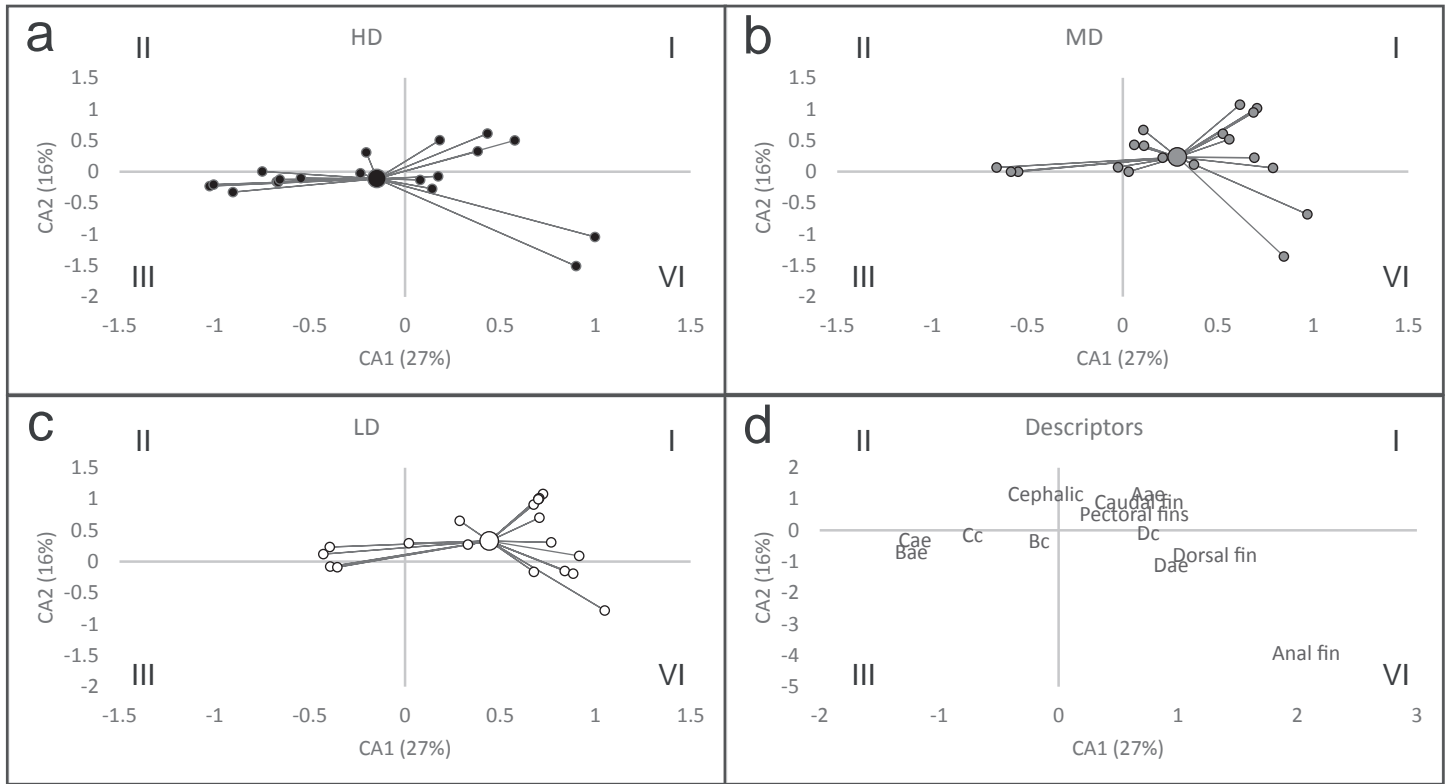


Figure 6



	<i>HD</i>		<i>MD</i>		<i>LD</i>	
	% anomalies	% affected specimens	% anomalies	% affected specimens	% anomalies	% affected specimens
<i>A4 red</i>	0.1	2				
<i>A4 elo</i>	0.1	2				
<i>A5</i>	2.4	23	1.2	9	3.5	26
<i>A18</i>	3.8	34	3.7	27	7.1	53
<i>A26</i>	2.1	15	3.1	13	2.8	16
<i>A30</i>					0.7	5
<i>B3 tot</i>	0.4	3				
<i>B4 def</i>	0.4	5	0.3	2		
<i>B4 red</i>					0.7	5
<i>B5 mis</i>	0.1	2				
<i>B5 bif</i>					1.4	5
<i>B5 sup</i>	0.1	2				
<i>B5 sup L</i>	0.1	2				
<i>B5 abs</i>	0.3	3				
<i>B5 abs L</i>	0.3	3				
<i>B5 abs R</i>	0.3	3			0.7	5
<i>B6</i>					0.7	5
<i>B6 abs</i>	0.4	5			0.7	5
<i>B7 bif</i>	0.1	2				
<i>B7 abs</i>	0.4	5				
<i>C2</i>			0.3	2		
<i>C3</i>	2.5	26	5.5	27	0.7	5
<i>C3 tot</i>	1.9	17	0.6	4		
<i>C4 def</i>	2.8	23	3.1	16	2.8	21
<i>C4 red</i>	2.3	17	1.8	9	2.8	21
<i>C5</i>	14.4	78	14.7	47	6.4	26
<i>C5 ins</i>	0.4	5				
<i>C5 mis</i>	1.2	11	0.9	7		
<i>C5 bif</i>	0.1	2			1.4	5
<i>C5 sup</i>	0.1	2				
<i>C5 sup L</i>	0.7	8	0.3	2	0.7	5
<i>C5 sup R</i>	0.7	6	0.3	2		
<i>C5 abs</i>	0.7	6	0.3	2		
<i>C5 abs L</i>	2.3	22	0.6	4	0.7	5
<i>C5 abs R</i>	3.2	28	1.8	13		
<i>C6</i>	15.9	78	14.7	47	8.5	21
<i>C6 ins</i>	1.2	11	0.6	4	0.7	5
<i>C6 mis</i>	0.4	5				
<i>C6 bif</i>	0.1	2			2.8	11
<i>C6 sup</i>	0.1	2				
<i>C6 sup L</i>	0.4	5				
<i>C6 sup R</i>	0.3	3	0.3	2		
<i>C6 abs</i>	2.1	18	1.5	9		

C6 abs L	3.3	31	0.9	7	1.4	11
C6 abs R	2.3	22	2.1	13	0.7	5
CS	0.1	2				
29	1.7	20	0.6	4	2.1	16
CL L			0.3	2		
E8 def	0.5	3				
E8 fus	0.1	2				
E11 def	0.3	2				
F8 def	5.7	25	1.8	9	2.1	11
F8 fus	0.1	2	0.3	2	0.7	5
F8 dec	0.3	2				
F11 sup					0.7	5
G9 def	1.9	15	11.0	38	8.5	32
G9 abs		0	0.3	2	1.4	11
G9 fus	0.1	2				
G9* dec	2.0	23	2.4	18	2.8	21
G9* def	0.4	5	0.3	2	2.1	16
G9* fus	0.5	6	1.8	13	3.5	26
G10 dec	3.3		6.1	2	6.4	
G10 def		38	0.3	44		47
G10 abs	0.1			2		
G10 fus		2	0.3			
G11 def	0.4	5	1.5	11	3.5	26
G19	9.5	71	12.2	71	14.9	74
H8 def	0.7	5	0.6	4	1.4	11
H8 sup					0.7	5
H11 def	1.1	6	0.6	2		
L11 def	0.1	2				
15				0	0.7	5
16	0.1	2	0.6	4		
17* def R	0.1	2				

Supplementary Table 1 The frequency of each anomalies and the frequency of specimens affected per each experimental group

Fig_1_SupplInfo

T0 specimens-survival rate

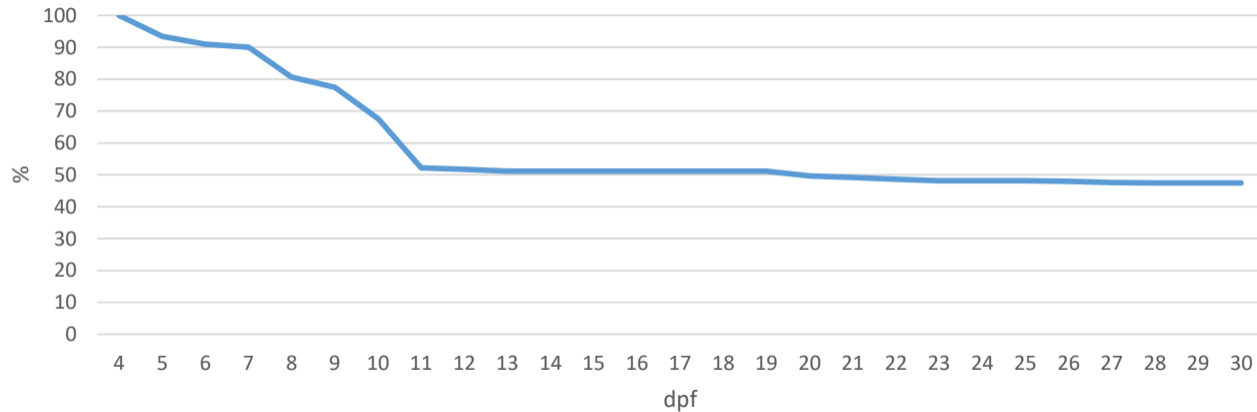


Figure_1_SupplInfo: Survival rate for the T0 samples